

A HUBBLE SPACE TELESCOPE CENSUS OF NUCLEAR STAR CLUSTERS IN LATE-TYPE SPIRAL GALAXIES. I. OBSERVATIONS AND IMAGE ANALYSIS¹

TORSTEN BÖKER,² SEPPO LAINE, AND ROELAND P. VAN DER MAREL

Space Telescope Science Institute, 3700 San Martin Drive, Baltimore, MD 21218; boeker@stsci.edu, laine@stsci.edu, marel@stsci.edu

MARC SARZI AND HANS-WALTER RIX

Max-Planck-Institut für Astronomie, Königstuhl 17, D-69117 Heidelberg, Germany; sarzi@mpia-hd.mpg.de, rix@mpia-hd.mpg.de

LUIS C. HO

Observatories of the Carnegie Institution of Washington, 813 Santa Barbara Street, Pasadena, CA 91101-1292; lho@ociw.edu

AND

JOSEPH C. SHIELDS

Department of Physics and Astronomy, Clippinger Research Laboratories, Ohio University, 251B, Athens, OH 45701-2979; shields@helios.phy.ohiou.edu

Received 2001 October 8; accepted 2001 December 4

ABSTRACT

We present new *Hubble Space Telescope* *I*-band images of a sample of 77 nearby late-type spiral galaxies with low inclination. The main purpose of this catalog is to study the frequency and properties of nuclear star clusters. In 59 galaxies of our sample, we have identified a distinct, compact (but resolved), and dominant source at or very close to the photocenter. In many cases, these clusters are the only prominent source within a few kiloparsecs from the galaxy nucleus. We present surface brightness profiles, derived from elliptical isophote fits, of all galaxies for which the fit was successful. We use the fitted isophotes at radii larger than $2''$ to check whether the location of the cluster coincides with the photocenter of the galaxy and confirm that in nearly all cases, we are truly dealing with “nuclear” star clusters. From analytical fits to the surface brightness profiles, we derive the cluster luminosities after subtraction of the light contribution from the underlying galaxy disk and/or bulge.

Key words: galaxies: nuclei — galaxies: spiral — galaxies: star clusters — galaxies: statistics — galaxies: structure

1. INTRODUCTION

Over the past decade, high dynamic range observations with modern CCD detectors have shown that compact stellar nuclei are a common feature of spiral galaxies of all Hubble types. For example, Matthews & Gallagher (1997) noticed 10 objects with compact nuclear star clusters in a survey of 49 southern, very late type spirals, while Philips et al. (1996) found unresolved, bright nuclei in six out of the 10 late-type spirals in their sample. However, as one progresses along the Hubble sequence toward earlier types, the increasingly luminous bulge component with its steeply rising surface brightness profile makes the identification of an additional unresolved cluster extremely difficult. It therefore took the unique spatial resolution of the *Hubble Space Telescope* (*HST*) to demonstrate that nuclear clusters are a common phenomenon also in earlier Hubble types (e.g., Carollo, Stiavelli, & Mack 1998). *HST* currently provides the only means to investigate the structural properties of nuclear star clusters, as demonstrated by Matthews et al.

(1999), and to cleanly separate their emission from the underlying galaxy disk/bulge.

Despite the recent progress, the formation mechanism of nuclear star clusters remains largely a mystery. Intuitively, there are good reasons to expect matter accumulation in the deep gravitational wells of galaxies with massive bulges and hence active star formation in their nuclei. In contrast, the gravitational force all but vanishes in the centers of pure disk galaxies with shallow surface brightness profiles and without any discernible bulge component. In these galaxies, the dynamical center is not a “special” place, and it is far from obvious how a massive stellar cluster could have formed there. The shallow gravitational potential might provide a natural explanation for the fact that spirals of late Hubble type are not known to contain supermassive black holes. On the other hand, nuclear star clusters can be extremely compact: the nucleus of M33, for example, has likely undergone core collapse and is as compact as any known globular cluster (Kormendy & McClure 1993). So far, no satisfying explanation has been put forward to explain the high gas densities that must have been present in the nuclei of these shallow disk galaxies to enable the formation of such massive and compact objects.

It is also unknown whether nuclear star clusters form repeatedly or only once—a question with important implications for the dynamical and morphological evolution of their host galaxies. To make progress along this line, it is essential to obtain the age distribution of nuclear star clus-

¹ Based on observations made with the NASA/ESA *Hubble Space Telescope*, obtained at the Space Telescope Science Institute, which is operated by the Association of Universities for Research in Astronomy, Inc., under NASA contract NAS 5-26555. These observations are associated with proposal 8599.

² Affiliated with the Astrophysics Division, Space Science Department, European Space Agency.

ters. So far, reliable age estimates exist for only a handful of nuclear star clusters. Interestingly, most of them appear to be rather young: our Galaxy has a central stellar cluster with an age of only ~ 3 Myr (Krabbe et al. 1995), and both M31 and M33 have blue nuclei that are very likely young star clusters (Lauer et al. 1998). More recently, we have published nuclear cluster ages derived from ground-based spectroscopy for IC 342 (≤ 60 Myr; Böker, van der Marel, & Vacca 1999) and NGC 4449 (6–10 Myr; Böker et al. 2001; Gelatt, Hunter, & Gallagher 2001). In addition, the dominant stellar population of the nuclear cluster in NGC 3227 is less than 50 Myr old (Schinnerer, Eckard, & Tacconi 2001).

However, it is possible (and in fact quite likely) that ground-based observations predominantly target the brightest and hence youngest clusters. In order to get a more representative picture of nuclear star clusters, it is important to study a galaxy sample that is free from selection effects that favor the high end of the nuclear cluster luminosity range. In this paper, we describe the results of an *HST* *I*-band imaging survey of an unbiased sample of nearby, face-on, very late type spirals (Scd or later). The main goals of the survey are to (1) determine the frequency of nuclear star clusters in very late type spirals, (2) derive their luminosity and size distribution, (3) compare their properties to those of nuclear star clusters in earlier Hubble types that have been more extensively studied with *HST* (Carollo et al. 1997, 1998, 1999, 2001), and (4) provide a source catalog for follow-up spectroscopic observations to age-date their stellar populations. The main purpose of this paper is to present the complete data set. In a companion paper (Böker et al. 2002a), we describe the statistics of the full sample and investigate whether the properties of nuclear star clusters correlate in any way with those of their host galaxies.

This paper is organized as follows: In § 2 we describe our sample selection criteria, the observational strategy, and the data reduction procedure, and we present the final images as well as the results of the isophotal analysis. In § 3 we discuss whether the clusters indeed occupy the nuclei of their host galaxies and how they compare to other luminous star clusters observed in a variety of starburst environments. We conclude in § 4.

2. SAMPLE SELECTION, OBSERVATIONS, AND DATA REDUCTION

2.1. The Sample

The target list for our survey was selected from the Third Reference Catalog of Bright Galaxies (de Vaucouleurs et al. 1991) according to the following criteria:

1. Hubble type between Scd and Sm ($6 \leq T \leq 9$).
2. Line-of-sight velocity $v_{\text{hel}} < 2000$ km s $^{-1}$ to assure good spatial resolution in physical units.
3. Axis ratio parameter $R_{25} \equiv \log(a/b) < 0.2$, i.e., inclination close to face-on. This helps to minimize the effects of dust extinction due to the galaxy disk and to avoid confusion in the identification of the nucleus from line-of-sight projection of disk clusters.

Our sample is unbiased with respect to galaxy size, mass, total magnitude, star formation efficiency, or any other quantity that might reasonably be expected to favor or dis-

favor nuclear cluster formation. It should therefore be well suited to provide an objective census of nuclear clusters in late-type galaxies in the local universe.

We identified a total of 113 galaxies that satisfied the above criteria and had not previously been observed with the Wide Field Planetary Camera 2 (WFPC2) on board *HST* in the F814W filter. These 113 galaxies were used as the target pool for our WFPC2 snapshot program (GO-8599). To date, 77 galaxies have been successfully observed, as listed in Table 1. It is possible that a few more targets will be observed later, but for this paper we limited the sample to those galaxies observed before 2001 August 3.

2.2. The WFPC2 Images

All images were taken with the WFPC2 camera on board *HST*, with the galaxy nucleus centered on the Planetary Camera (PC) chip. The PC pixel size is $0''.0464$, and the field of view is $36'' \times 36''$. We used the F814W filter with an integration time of 600 s, split into two exposures of 300 s to allow cosmic-ray rejection. We also took a short exposure (40 s) to guard against saturation of the WFPC2 detectors in the 300 s exposures. However, none of the galaxies was bright enough to require the use of the 40 s exposure. The point-spread function (PSF) with the F814W filter has a full-width at half maximum (FWHM) of $0''.07$.

We used the STSDAS task *wfixup* to interpolate (in the *x*-direction) over bad pixels as identified in the data quality files. We also used the STSDAS task *warmpix* to correct consistently warm pixels in the data, using the most recent warm-pixel tables that are provided by the WFPC2 instrument group at the Space Telescope Science Institute about once a month. The STSDAS task *cceej* was used to combine the two 300 s exposures. This step corrects most of the pixels affected by cosmic rays in the combined image. In general, a few cosmic rays remain uncorrected, mostly when the same pixel was hit in both exposures. Also, a small number of hot pixels remain uncorrected because they are not listed even in the most recent warm-pixel tables. We corrected these with the IRAF task *cosmicrays*, setting the “threshold” and “fluxratio” parameters to suitable values that were selected by careful comparison of the images before and after correction to ensure that only questionable pixels were replaced. The photometric calibration and conversion to a Johnson *I* band was performed according to Holtzman et al. (1995). We assumed a standard color of $V-I = 1$ for the galaxies, which translates into a zero point of 21.55 (note that the assumed color affects the zero point only weakly: a color of $V-I = 2$ would result in a zero point of 21.56).

After visual inspection of the images, we divided the objects into two groups. The first group contains those 59 objects for which (1) the (photo)center of the galaxy is reasonably well defined, and (2) a prominent, isolated pointlike source can be identified close to it. These sources are nuclear cluster candidates. In § 3.1 we discuss our criteria for whether they are indeed occupying the photocenter or not.

The second group contains the remaining 18 galaxies, which show no easily identifiable source close to the center. This does not necessarily mean that these galaxies do not harbor a nuclear cluster; it merely indicates that we cannot identify one with any kind of certainty from our data.

Figures 1 and 2 contain the images of the 59 galaxies in group 1 and the 18 galaxies in group 2, respectively. Visual

TABLE 1
SUMMARY OF OBSERVATIONS

Galaxy (1)	R.A. (J2000.0) (2)	Decl. (J2000.0) (3)	v_z (km s ⁻¹) (4)	Type (5)	m_B (mag) (6)	A_I (mag) (7)	d_{MA} (arcmin) (8)	Observation Date (9)
NGC 275	00 51 04.20	-07 04 00.0	1681	SB(rs)cd pec	13.16	0.109	1.5	2001 Jul 9
NGC 300	00 54 53.47	-37 41 00.0	-54	SA(s)d	8.95	0.025	21.9	2001 May 6
NGC 337a.....	01 01 33.90	-07 35 17.7	998	SAB(s)dm	14.92	0.189	5.9	2001 Jul 10
NGC 428	01 12 55.60	-00 58 54.4	1130	SAB(s)m	11.91	0.055	4.1	2001 Jan 6
NGC 450	01 15 30.52	-00 51 38.3	1720	SAB(s)cd:	12.20	0.077	3.1	2001 Jul 12
ESO 80-6.....	01 47 16.87	-62 58 14.8	1227	SB(s)m	14.37	0.052	1.4	2001 Jul 10
NGC 600	01 33 05.25	-07 18 42.1	1763	SB(rs)d	13.65	0.073	3.3	2001 Jul 9
NGC 853	02 11 43.35	-09 18 01.1	1413	Sm pec	13.43	0.050	1.5	2000 Jul 10
NGC 1042.....	02 40 23.63	-08 25 59.8	1271	SAB(rs)cd	12.50	0.056	4.7	2001 Jan 26
NGC 1313.....	03 18 15.37	-66 29 50.6	174	SB(s)d	9.20	0.212	9.1	2001 Jan 12
ESO 358-5.....	03 27 16.47	-33 29 06.1	1409	SAB(s)m pec:	14.90	0.022	1.4	2001 May 31
ESO 418-8.....	03 31 30.48	-30 12 44.6	988	SB(r)d	13.68	0.029	1.2	2001 May 30
NGC 1493.....	03 57 27.73	-46 12 38.1	796	SB(rs)cd	11.78	0.020	3.5	2001 May 2
ESO 202-41.....	04 36 56.69	-52 10 25.2	1396	SB(s)m	14.94	0.017	1.2	2001 Apr 27
ESO 85-47.....	05 07 43.86	-62 59 24.3	1180	SB(s)m	14.53	0.050	1.7	2001 Apr 26
ESO 204-22.....	05 36 26.06	-52 11 02.5	1005	SB(s)m: pec	15.44	0.080	1.3	2000 Dec 25
NGC 2139.....	06 01 07.90	-23 40 21.3	1649	SAB(rs)cd	11.99	0.065	2.6	2001 Jan 15
UGC 3574.....	06 53 10.60	+57 10 39.0	1635	SA(s)cd	13.20	0.103	4.2	2001 Jan 30
UGC 3826.....	07 24 32.05	+61 41 35.2	1946	SAB(s)d	14.10	0.133	3.5	2000 Oct 6
NGC 2552.....	08 19 20.14	+50 00 25.2	695	SA(s)m?	12.56	0.090	3.5	2001 Apr 6
UGC 4499.....	08 37 41.43	+51 39 11.1	877	SA dm	13.50	0.069	2.6	2001 May 31
NGC 2763.....	09 06 49.26	-15 29 59.9	1769	SB(r)cd pec	12.64	0.141	2.3	2001 Apr 2
NGC 2805.....	09 20 24.56	+64 05 55.2	1968	SAB(rs)d	11.52	0.100	6.3	2000 Oct 7
UGC 4988.....	09 23 15.26	+34 44 03.7	1696	SABm	15.30	0.036	1.1	2001 Jun 3
UGC 5015.....	09 25 47.89	+34 16 35.9	1800	SABdm	14.90	0.034	1.9	2001 Jun 4
UGC 5288.....	09 51 17.00	+07 49 39.0	559	Sdm:	14.09	0.066	1.3	2001 Jan 14
NGC 3206.....	10 21 47.65	+56 55 49.6	1380	SB(s)cd	12.57	0.027	3.0	2001 May 14
NGC 3346.....	10 43 38.90	+14 52 18.0	1315	SB(rs)cd	12.41	0.054	2.9	2001 Jan 14
NGC 3423.....	10 51 14.30	+05 50 24.0	1025	SA(s)cd	11.59	0.058	3.8	2001 Feb 7
NGC 3445.....	10 54 35.87	+56 59 24.4	2245	SAB(s)m	12.90	0.015	1.6	2001 Jun 1
NGC 3782.....	11 39 20.72	+46 30 48.6	944	SAB(s)cd:	13.10	0.035	1.7	2001 May 10
NGC 3906.....	11 49 40.46	+48 25 33.3	1166	SB(s)d	13.49	0.050	1.9	2001 Mar 9
NGC 3913.....	11 50 38.77	+55 21 12.1	1190	SA(rs)d:	13.17	0.025	2.6	2001 Jan 17
A 1156+52.....	11 59 09.47	+52 42 26.1	1307	SB(rs)cd	13.12	0.053	3.5	2001 Aug 3
ESO 504-30.....	11 57 15.14	-27 42 00.2	1673	SB(r)d:	14.66	0.142	1.1	2001 May 6
UGC 6931.....	11 57 22.79	+57 55 22.5	1446	SBm:	14.31	0.049	1.4	2000 Aug 16
NGC 4027.....	11 59 30.50	-19 15 44.0	1588	SB(s)dm	11.66	0.081	3.2	2001 Apr 7
NGC 4204.....	12 15 14.51	+20 39 30.7	968	SB(s)dm	12.90	0.065	3.6	2001 Jun 11
NGC 4299.....	12 21 40.90	+11 30 03.0	306	SAB(s)dm:	12.88	0.063	1.7	2001 Apr 28
NGC 4416.....	12 26 46.72	+07 55 07.9	1449	SB(rs)cd:	13.14	0.049	1.7	2001 Mar 19
NGC 4411B.....	12 26 47.30	+08 53 04.5	1334	SAB(s)cd	12.91	0.058	2.5	2001 May 28
NGC 4487.....	12 31 04.36	-08 03 13.8	1020	SAB(rs)cd	12.26	0.041	4.2	2001 May 28
NGC 4496A.....	12 31 39.32	+03 56 22.7	1772	SB(rs)m	11.94	0.048	4.0	2001 Mar 17
NGC 4517A.....	12 32 28.15	+00 23 22.8	1554	SB(rs)dm:	12.94	0.046	4.0	2001 Mar 18
NGC 4540.....	12 34 50.90	+15 33 06.9	1383	SAB(rs)cd	12.44	0.065	1.9	2001 Jul 19
NGC 4618.....	12 41 32.74	+41 09 03.8	748	SB(rs)m	11.22	0.041	4.2	2001 Jul 10
NGC 4625.....	12 41 52.61	+41 16 26.3	816	SAB(rs)m pec	12.92	0.035	2.2	2001 May 28
NGC 4701.....	12 49 11.71	+03 23 21.8	768	SA(s)cd	12.80	0.057	2.8	2001 May 29
NGC 4775.....	12 53 45.79	-06 37 20.1	1565	SA(s)d	12.24	0.067	2.1	2000 Dec 21
NGC 4904.....	13 00 56.97	-00 01 31.9	1204	SB(s)cd	12.60	0.050	2.2	2000 Jul 12
A 1301-03.....	13 04 31.43	-03 34 20.3	1379	SAB(s)dm	12.90	0.058	3.5	2001 Jun 2
IC 4182	13 05 49.53	+37 36 17.6	515	SA(s)m	13.0	0.027	6.0	2001 Jul 9
ESO 444-2.....	13 16 44.91	-27 53 09.7	1544	SAB(s)dm	14.97	0.142	1.1	2001 May 30
NGC 5068.....	13 18 54.60	-21 02 19.7	607	SB(s)d	10.52	0.197	7.2	2001 Jun 2
UGC 8516.....	13 31 52.50	+20 00 01.0	1156	Scd:	14.03	0.057	1.1	2001 Jun 1
ESO 510-59.....	14 04 46.43	-24 49 40.7	2267	SB(s)cd	13.61	0.138	2.5	2001 Apr 27
NGC 5477.....	14 05 31.25	+54 27 12.3	565	SA(s)m	14.36	0.021	1.7	2001 Sep 22
NGC 5585.....	14 19 48.08	+56 43 43.8	571	SAB(s)d	11.20	0.030	5.8	2001 May 5
NGC 5584.....	14 22 23.65	-00 23 09.2	1695	SAB(rs)cd	12.63	0.075	3.4	2001 Apr 18
NGC 5668.....	14 33 24.30	+04 27 02.0	1665	SA(s)d	12.2	0.071	3.3	2001 Apr 23
NGC 5669.....	14 32 44.00	+09 53 31.0	1481	SAB(rs)cd	12.03	0.053	4.0	2001 Jul 14
NGC 5774.....	14 53 42.60	+03 34 59.0	1648	SAB(rs)d	12.74	0.081	3.0	2001 May 20
NGC 5789.....	14 56 35.52	+30 14 02.5	2002	Sdm	14.70	0.041	0.9	2001 Mar 17

TABLE 1—*Continued*

Galaxy (1)	R.A. (J2000.0) (2)	Decl. (J2000.0) (3)	v_z (km s ⁻¹) (4)	Type (5)	m_B (mag) (6)	A_I (mag) (7)	d_{MA} (arcmin) (8)	Observation Date (9)
NGC 5964.....	15 37 36.30	+05 58 26.0	1552	SB(rs)d	12.6	0.113	4.2	2001 May 2
ESO 138-10.....	16 59 02.96	-60 12 02.9	942	SA(s)cd	11.59	0.427	5.6	2001 May 29
NGC 6509.....	17 59 25.36	+06 17 12.4	1926	Sd	13.10	0.375	1.6	2001 Jul 3
NGC 6946.....	20 34 52.34	+60 09 14.2	310	SAB(rs)cd	9.61	0.663	11.5	2000 Dec 3
ESO 187-51.....	21 07 33.09	-54 57 02.0	1158	SB(s)m	14.85	0.066	1.9	2001 Mar 23
UGC 12082.....	22 34 11.54	+32 52 10.3	974	Sm	14.1	0.185	2.6	2001 Aug 13
NGC 7418.....	22 56 36.00	-37 01 47.3	1287	SAB(rs)cd	12.30	0.031	3.5	2001 Jun 1
NGC 7424.....	22 57 18.08	-41 04 19.0	765	SAB(rs)cd	10.96	0.021	9.5	2001 Jun 1
ESO 290-39.....	23 03 29.14	-46 02 22.8	1337	SB(s)m	15.0	0.028	1.1	2001 Oct 12
UGC 12732.....	23 40 39.80	+26 14 10.0	870	Sm:	13.8	0.172	3.0	2001 May 14
ESO 241-6.....	23 56 13.08	-43 26 00.0	1219	SB(s)m	14.4	0.025	1.1	2000 Nov 12
NGC 7689.....	23 33 16.11	-54 05 37.0	1744	SA(r)c	12.2	0.023	2.9	2001 Jul 12
NGC 7741.....	23 43 53.65	+26 04 33.1	872	SB(s)cd	11.84	0.145	4.4	2001 Jul 24
NGC 7793.....	23 57 49.75	-32 35 29.5	69	SA(s)d	9.98	0.038	9.3	2001 Apr 19

NOTE.—Cols. (1)–(3): Object name and coordinates, as taken from NED. Units of right ascension are hours, minutes, and seconds, and units of declination are degrees, arcminutes, and arcseconds. Col. (4): Recession velocity, corrected according to the Virgo-centric infall model (Sandage & Tammann 1990), taken from LEDA. Cols. (5) and (6): Galaxy morphological type and apparent total B magnitude (NED). Col. (7): Galactic foreground extinction (Schlegel, Finkbeiner, & Davis 1998), converted to I band using the Cardelli, Clayton, & Mathis 1989 extinction law, and $R_V = 3.1$ (NED). Col. (8): Galaxy major axis diameter (NED). Col. (9): Date of observation.

inspection of the images reveals a number of noteworthy points:

1. In most cases, the nuclear star cluster candidate is obvious in the images because it is the dominant source at or close to the photocenter of the galaxy. It is often (but not always) the brightest source in the field and in many cases is the only cluster within a kiloparsec from the photocenter.

2. For the vast majority of the sample galaxies, the images show no morphological evidence for a stellar bulge. While our sample was obviously selected to avoid bright stellar bulges, it is still surprising that there appear to be no bulges at all in many late-type spirals. The visual impression is confirmed by the surface brightness analysis in § 2.3. Our data set is uniquely suited for a detailed investigation of the structural properties of late-type spiral galaxies, which is, however, beyond the scope of this paper. We defer a more detailed study of the disk surface brightness, the (lack of) evidence for stellar bulges, and possible correlations with nuclear cluster properties to a later paper (Böker et al. 2002b).

3. In many cases (e.g., UGC 3574, UGC 5015, or NGC 4411B), the nuclear cluster is “naked”: it forms a distinct entity that appears completely isolated within the disk. The cluster location does not appear to be a dynamically “special” place because there are no spiral arms, dust lanes, or other signs of a kinematic center visible in the images. This is even true at the smallest spatial scales as observed in the most nearby galaxies, such as NGC 300 or NGC 7793. This confirms a notion by Matthews et al. (1999), who studied a sample of four extreme late-type spirals also with WFPC2.

4. In other cases (e.g., NGC 853, NGC 2139, or NGC 4027), however, the cluster location seems to be the origin of spiral structure or prominent dust lanes, indicative of it being at the dynamical center of the galaxy. If the mechanisms that lead to such a morphology are in any way connected to the presence of a nuclear cluster, it appears that they are a consequence rather than the prerequisite of

nuclear cluster formation because it is difficult to imagine how a galaxy like NGC 2139 can change its structure back to the smooth and regular appearance of those with “naked” nuclear clusters.

2.3. Isophotal Fits

We used the IRAF task *ellipse* to obtain surface brightness profiles (SBPs) over the PC field of view for all galaxies in our sample. For the galaxies in group 1, we started the fitting process centered on the cluster with a semimajor axis (SMA) length of 5 pixels (0".23). We varied the SMA length logarithmically (with a 15% step size), first going out to a maximum SMA of 350 pixels ($\approx 16''$), then inward to the sampling limit (SMA of 0.5 pixels, or 0".023). Throughout the fit, the ellipse center, ellipticity, and position angle were allowed to vary freely. By comparing the position of the peak surface brightness (i.e., the position of the putative nuclear cluster) to the center of the outer isophotes, we were able to decide whether the cluster indeed occupies the photocenter of the galaxy. This is further discussed in § 3.1.

For a small number of galaxies, such an unconstrained fit failed for a small range of radii, typically because of a complex morphology, a shallow surface brightness gradient, a low signal-to-noise ratio, or any combination of these factors. In these cases, we performed two fits: one fit as described above and going out as far as possible and a second fit starting at a large radius and going inward as far as possible. By combining the two fits, we were able to construct the SBP over most of the radial range, with data missing for only a few radii. For another small group of galaxies, we were forced to increase the spacing between isophotes (step size of 50%) to overcome the low signal-to-noise ratio.

The 18 galaxies in group 2 have no plausible candidate for a nuclear cluster. These are mostly objects with very low surface brightness and an ill-defined photocenter. In these cases, we proceeded as follows: We first derived an estimate for the photocenter and ellipticity of the galaxy from the average of three isophotes at large radii (typically 200 pixels

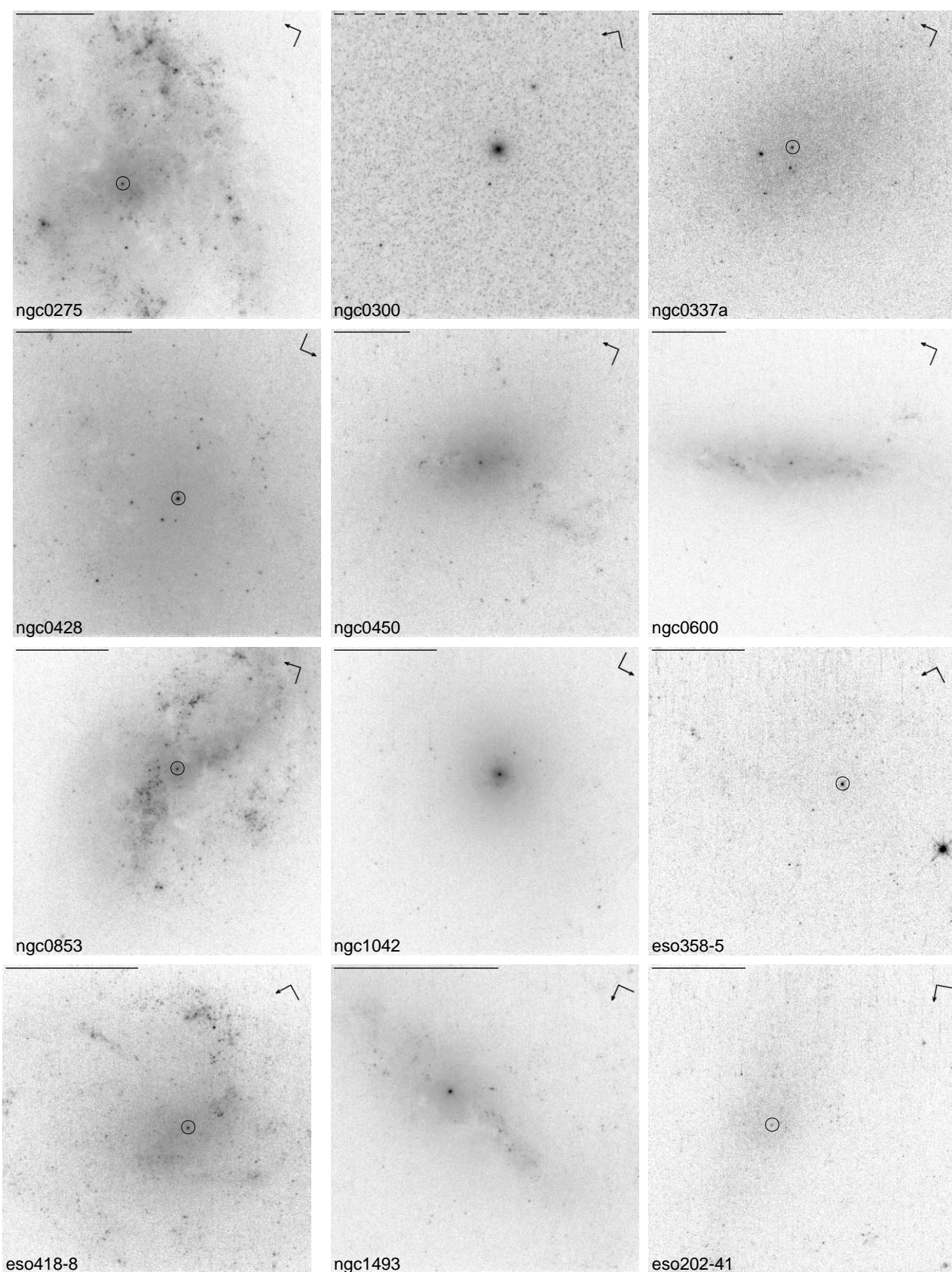


FIG. 1.—WFPC2 F814W images of the 59 galaxies with evidence for a nuclear cluster. Bars in upper left corners represent a scale of 1 kpc, calculated from the distances listed in Table 2. For a few very nearby objects, the bar is dashed, in which case it indicates a scale of 250 pc. Symbol in top right corner indicates north (*arrow*) and east directions. All images are on a logarithmic gray-scale stretch, optimized for the dynamic range of the galaxy. Objects identified as the central clusters are circled in sources where a visual identification may be ambiguous.

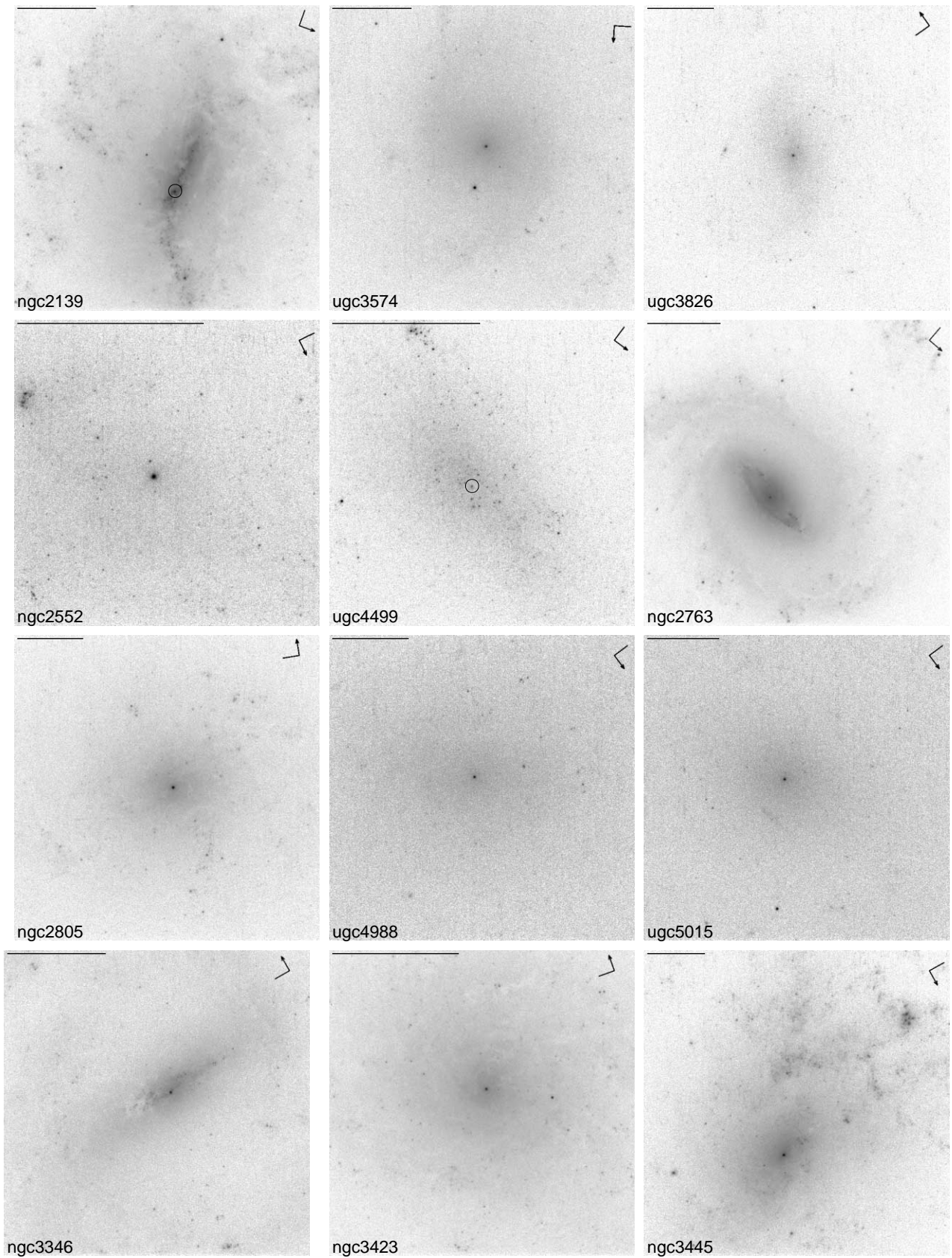


FIG. 1.—*Continued*

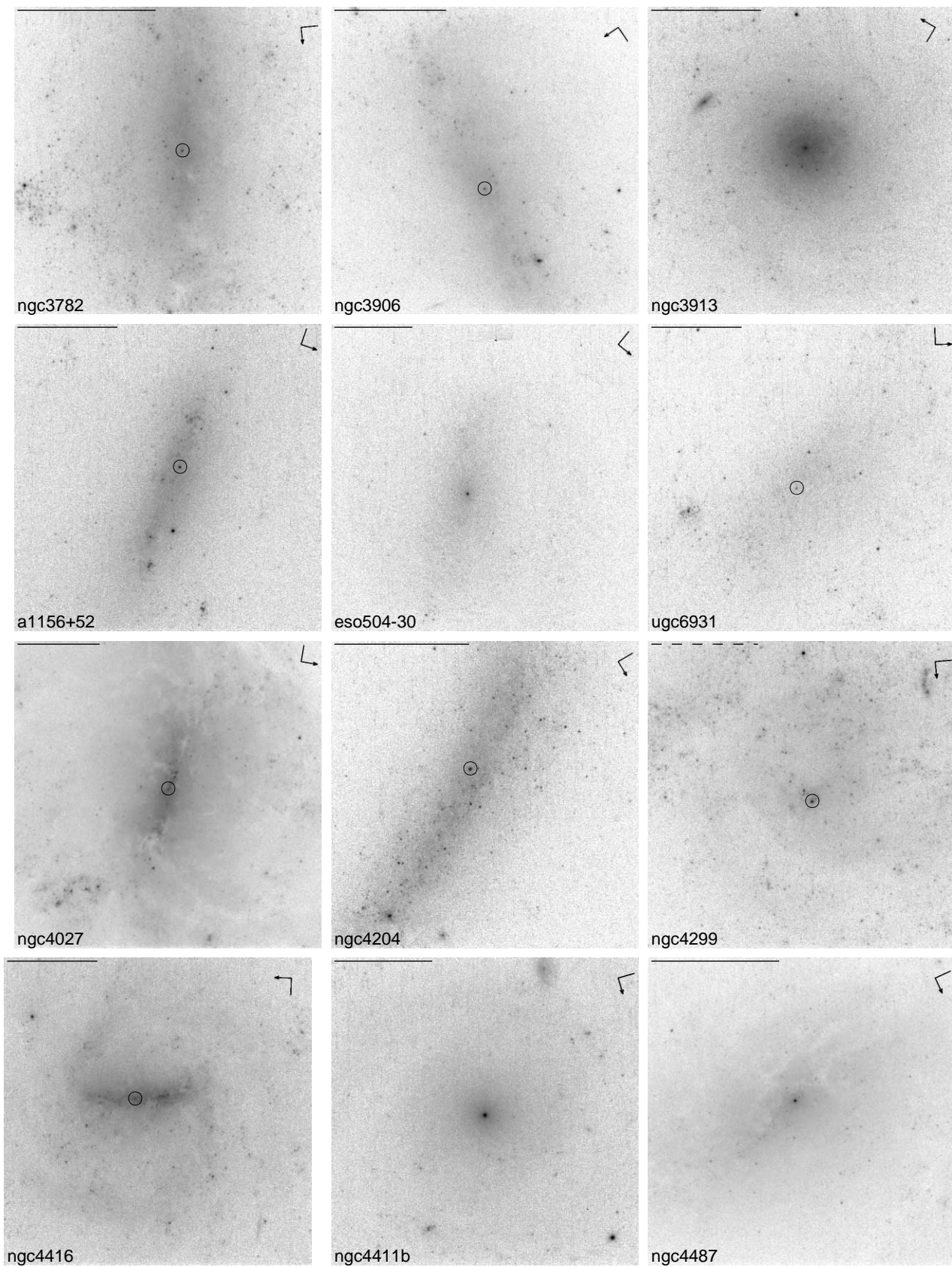


FIG. 1.—*Continued*

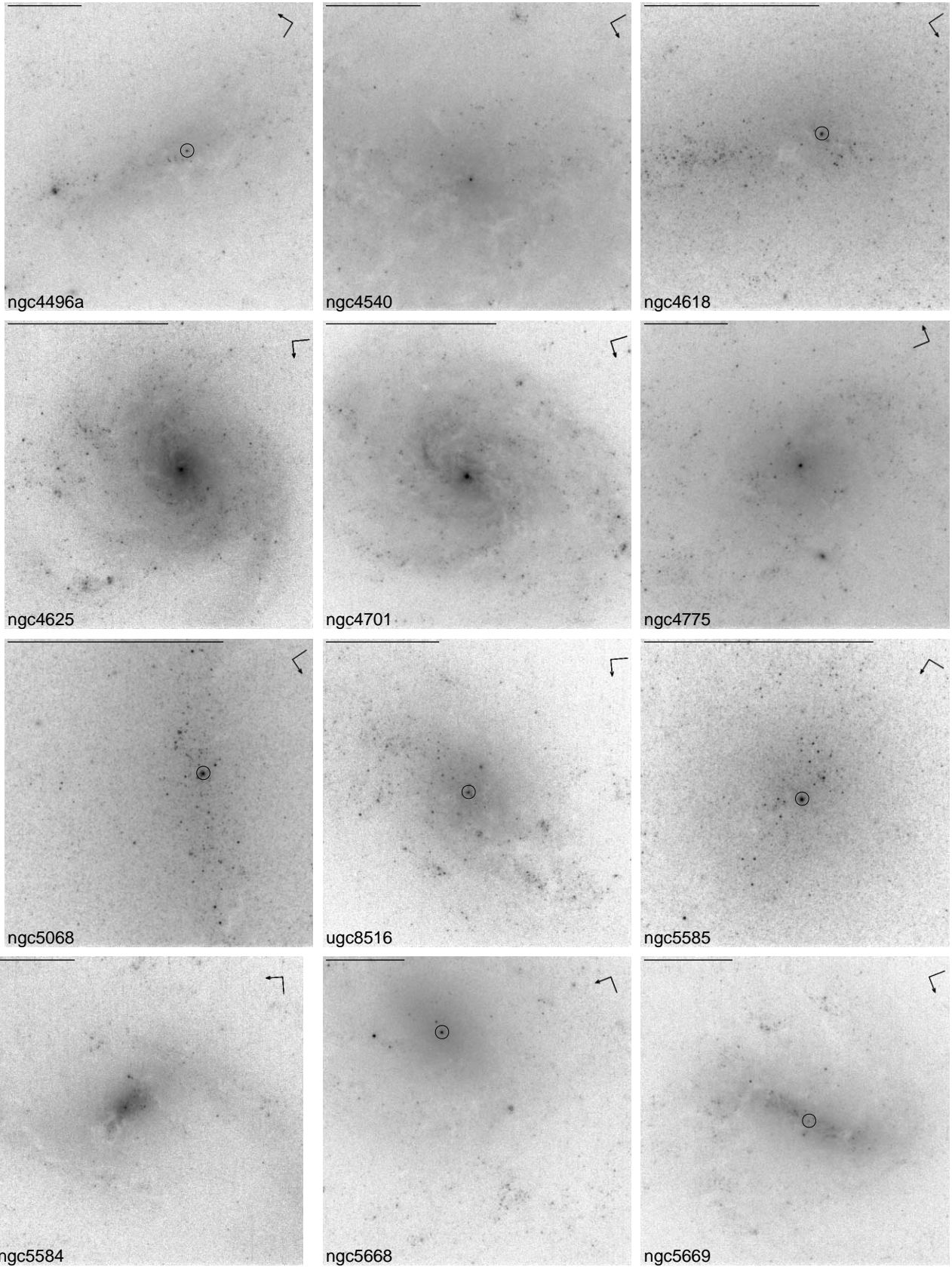


FIG. 1.—Continued

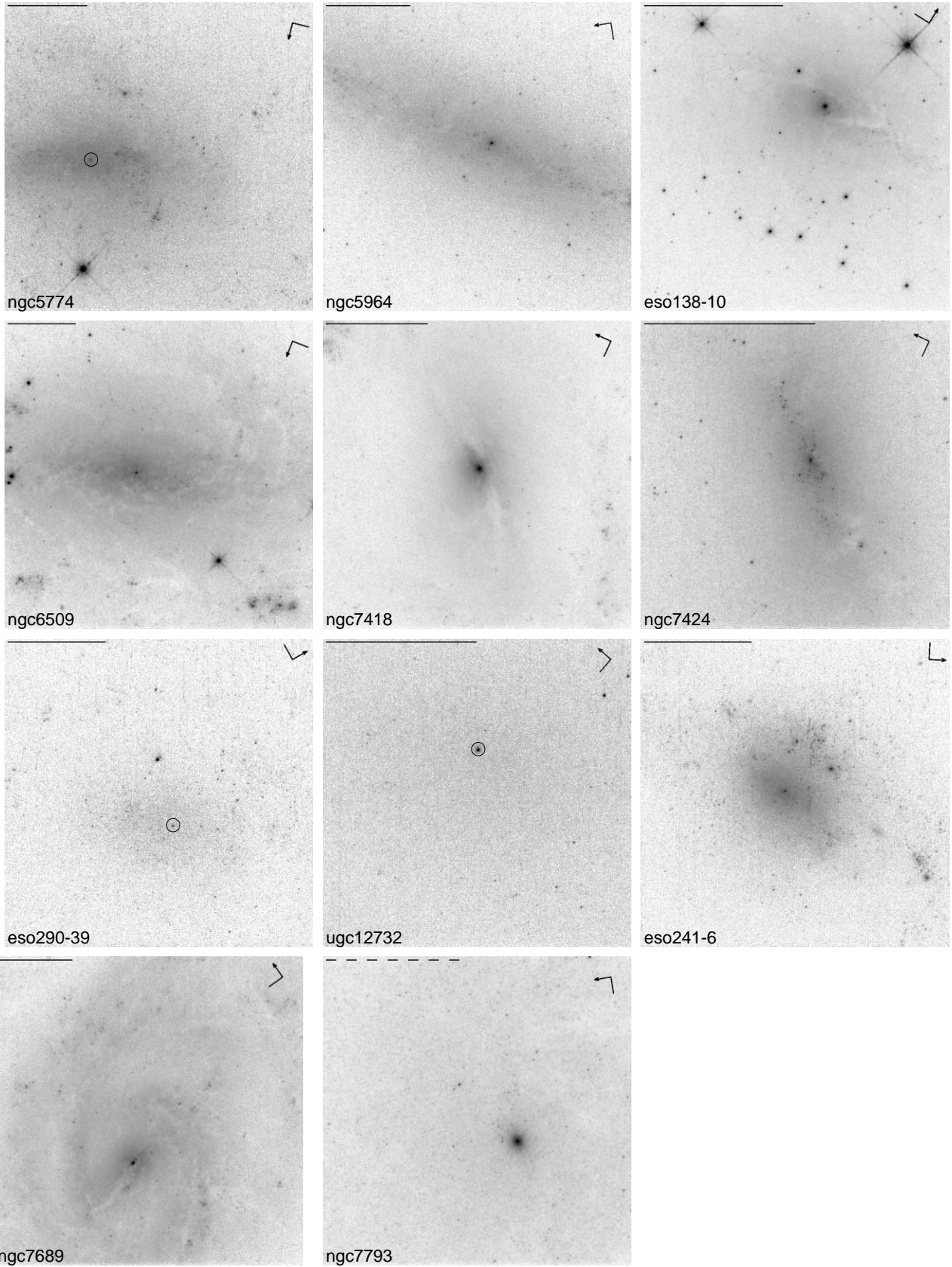


FIG. 1.—Continued

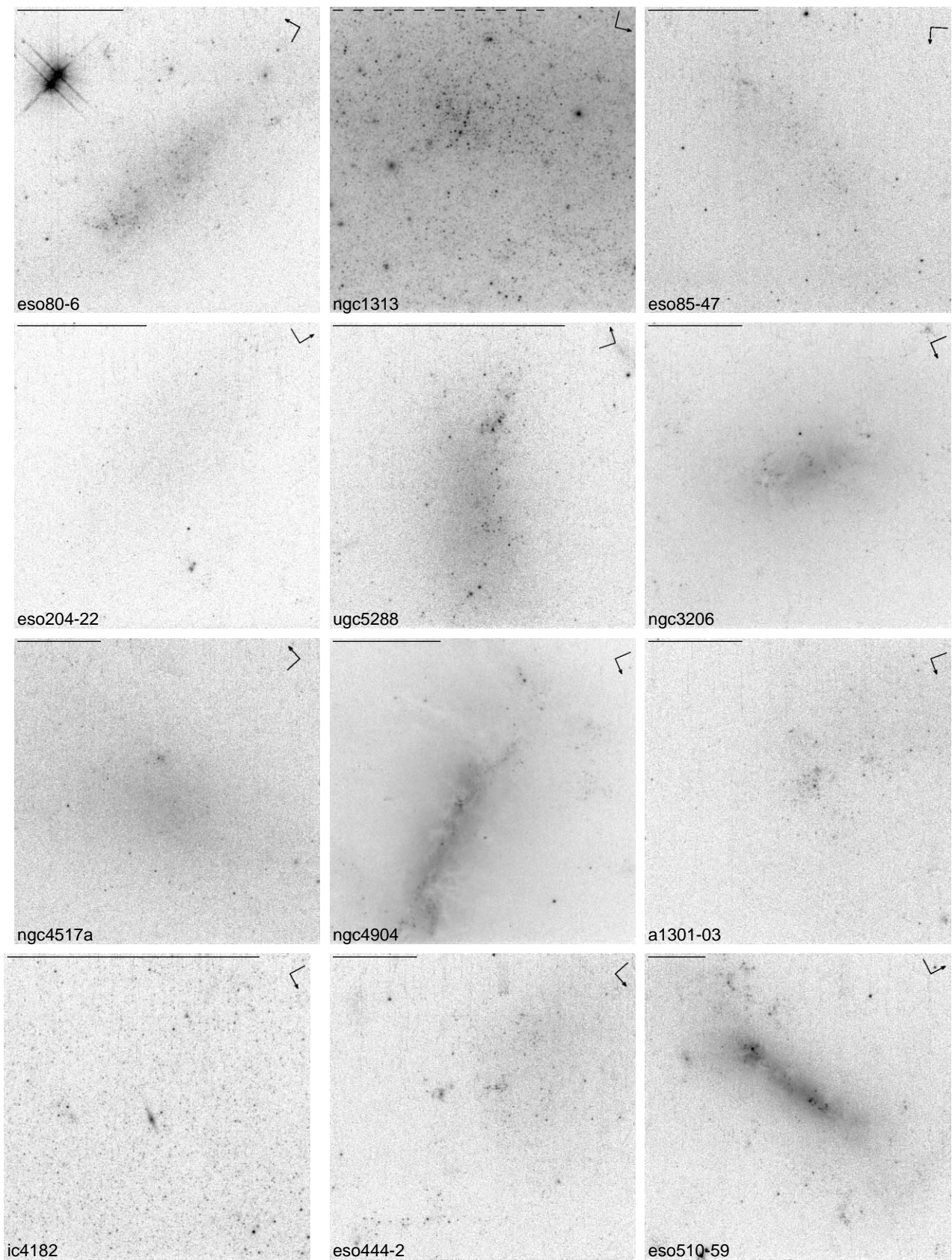


FIG. 2.—Same as Fig. 1, but for the 18 galaxies without evidence for a nuclear cluster

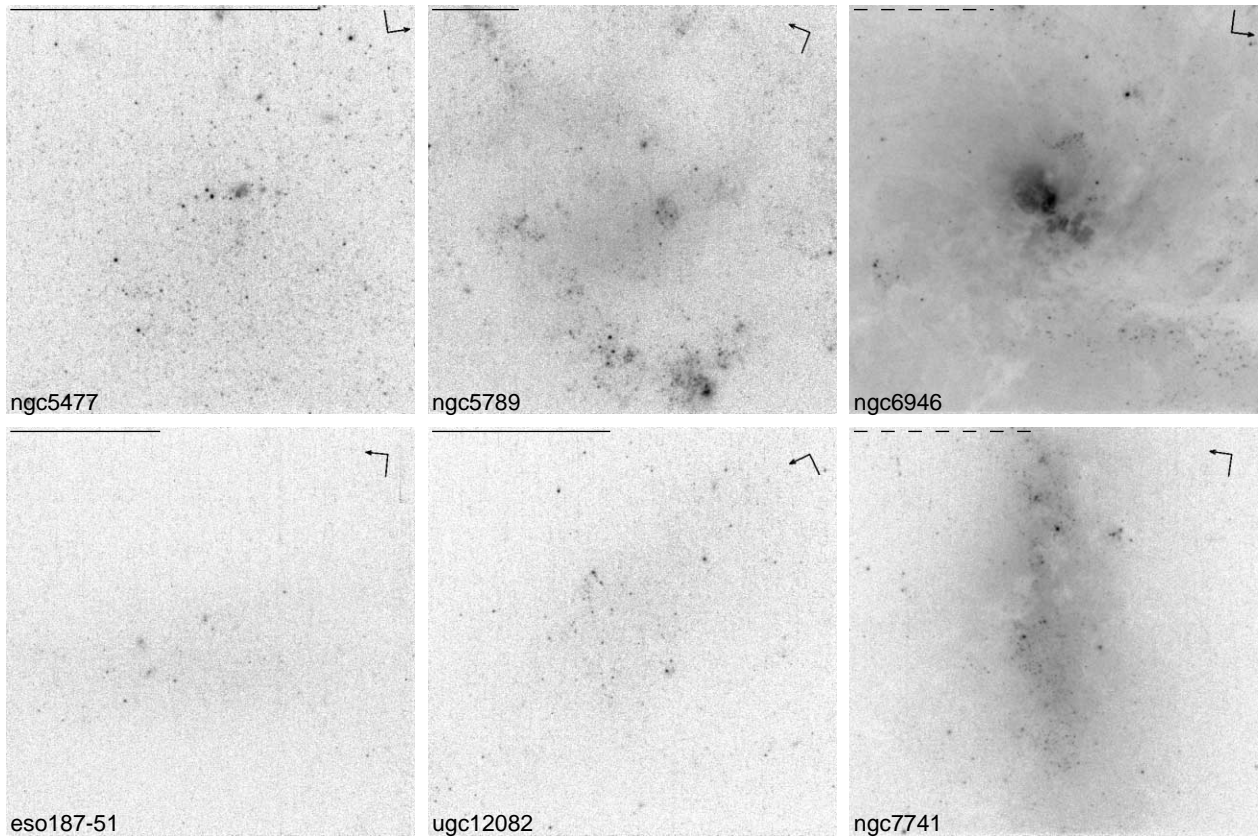


FIG. 2.—Continued

$\pm 15\%$). The SBP was then derived from a second fit, for which the isophote center and ellipticity was fixed to the initial estimates. This procedure worked for all but four galaxies, for which it was impossible to obtain even an estimate for the photocenter. One of these (ESO 510-59) appears to be a merger pair, one (NGC 6946) contains large amounts of dust in the nucleus, and the other two (A 1301-03 and IC 4182) are too faint in our images to detect a meaningful surface brightness gradient.

In Figures 3 and 4 we show the resulting SBPs for all galaxies in groups 1 and 2, respectively. The presence of the nuclear cluster candidate is obvious by the sharp upturn in the SBPs of Figure 3, typically at radii of around $0''.3$.

Not surprisingly, the clear upturn is absent in the profiles of the group 2 galaxies in Figure 4. Their SBPs are in general noisier and in some cases even decrease in brightness toward the center, just another manifestation of their shallow surface brightness gradients.

2.4. Photometry of the Nuclear Clusters

For the derivation of the luminosity of the nuclear clusters, it is useful to have a parametrized fit to the SBP. For this, we used the form

$$I(r) = I_0 \left(\frac{r}{r_b} \right)^{-\gamma} \left[1 + \left(\frac{r}{r_b} \right)^\alpha \right]^{(\gamma-\beta)/\alpha} \left[1 + \left(\frac{r}{r_c} \right)^\delta \right]^{(\beta-\epsilon)/\delta}. \quad (1)$$

This is based on the so-called nuker-law parametrization (Lauer et al. 1995; Byun et al. 1996), which represents a broken power law with an inflection point at a radius r_b . We

added an additional factor that allows for the possibility of a second inflection point at a radius r_c . The resulting equation was found to be sufficiently general for the purposes of this paper.

In general, the presence of a nuclear cluster causes a distinct upturn in the SBP at a certain radius R_u . This radius was identified by eye for each galaxy; the adopted values are listed in column (5) of Table 2. To estimate the cluster luminosity, we started by fitting the parametrization (1) to the data inside R_u (Fig. 3, *dotted curves*), followed by integration over an aperture with radius R_u . To obtain an estimate for the nuclear cluster luminosity, one needs to subtract from this the light contribution of the galaxy disk (and possibly bulge) within R_u . To this end, we considered two models for the SBP of the underlying galaxy light within the PC field of view that are likely to bracket the true SBP of the galaxy. For the first model, we assumed that the underlying galaxy has a constant surface brightness inside R_u (Fig. 3, *dashed lines*). For the second model, we performed a fit of a nuker law to the data outside R_u and extrapolated that fit to radii inside R_u (Fig. 3, *solid curves*).

After subtraction of the integrated luminosity inside R_u of the two models for the underlying galaxy light, we obtain two different estimates for the nuclear cluster luminosity. In Table 2, we list the mean of these two estimates and also half their difference as a measure of the uncertainty. The latter uncertainty indicates only the extent to which the cluster photometry depends on the choice of underlying galaxy model. In general, this is not the dominant source of error. The uncertainty due to the exact choice of the aperture size

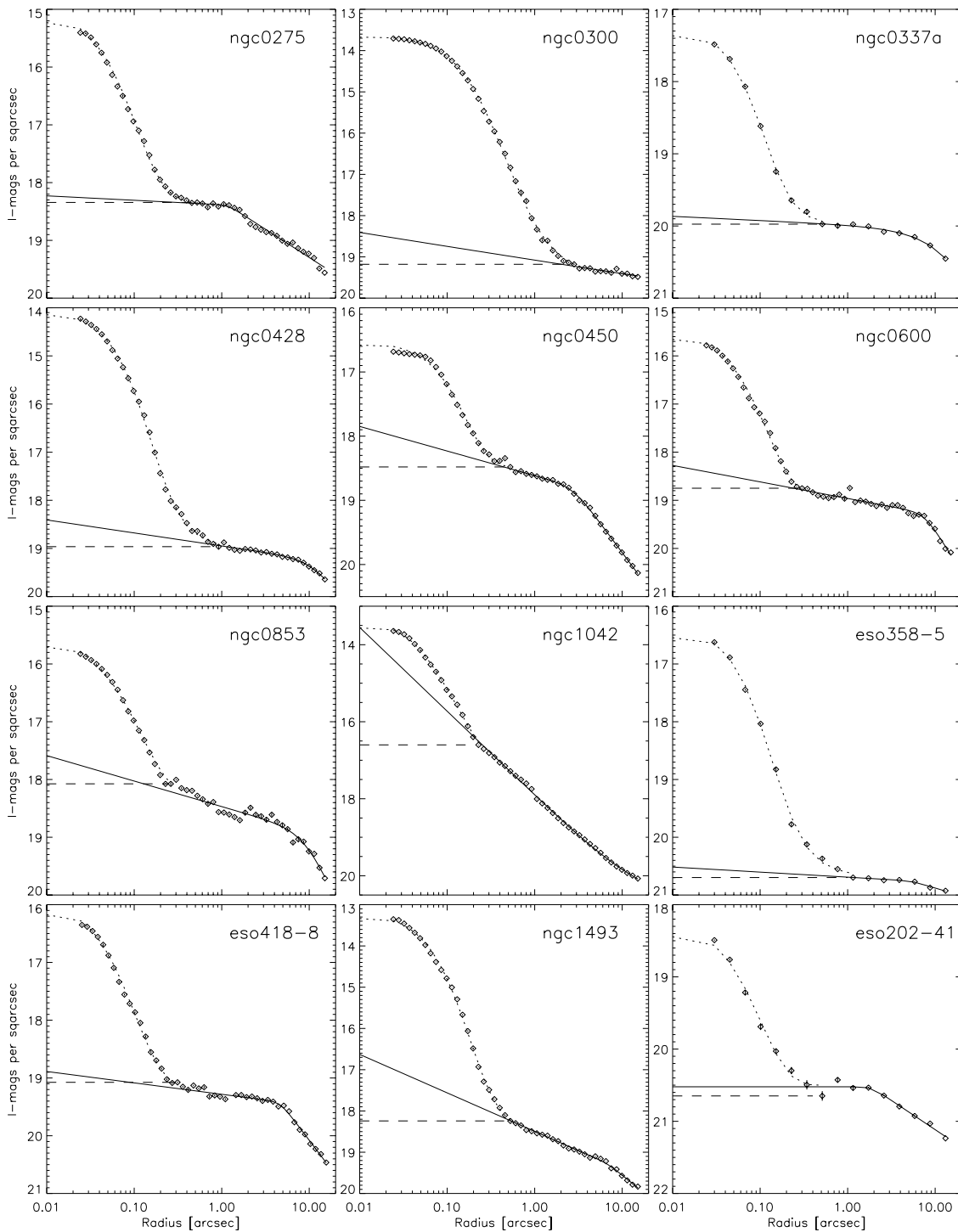


FIG. 3.—The I -band SBPs of the 59 galaxies with evidence for a nuclear cluster. Diamonds indicate the results of the elliptical isophote fits. Formal error bars of the isophote fits are also shown; in most cases, they are contained within the symbol. *Dotted lines*, best-fit analytical model to the inner part of the SBP as described in § 2; *solid lines*, inward-extrapolated best fit outside of the nuclear cluster; and *dashed lines*, the constant surface brightness level at the radius where the SBP starts to deviate from the pure disk profile. This radius was used to derive the cluster luminosity as described in § 2.4.

R_u adds at least 0.1 mag of error to the nuclear cluster luminosity estimates.

In Figure 5, we plot histograms of both apparent and absolute cluster luminosity. The distribution has a FWHM of about 4 mag, with a median of $M_I = -11.5$. This is brighter than even the brightest globular cluster in the Milky Way but is comparable to the bright end of the cluster luminosity function in the NGC 4038/4039 merging system (Whitmore

et al. 1999) or the young super star clusters in M82 (O’Connell et al. 1995). An absolute luminosity of $M_I = -11.5$ corresponds to $1.6 \times 10^6 L_\odot$ in the I band (because $M_{I,\odot} = 4.02$). The associated mass depends on the unknown mass-to-light ratio M/L . For reference, one can consider the case of a cluster formed in an instantaneous burst with a Salpeter (1955) initial mass function and solar metallicity. For a young cluster with an age of 10 Myr, one

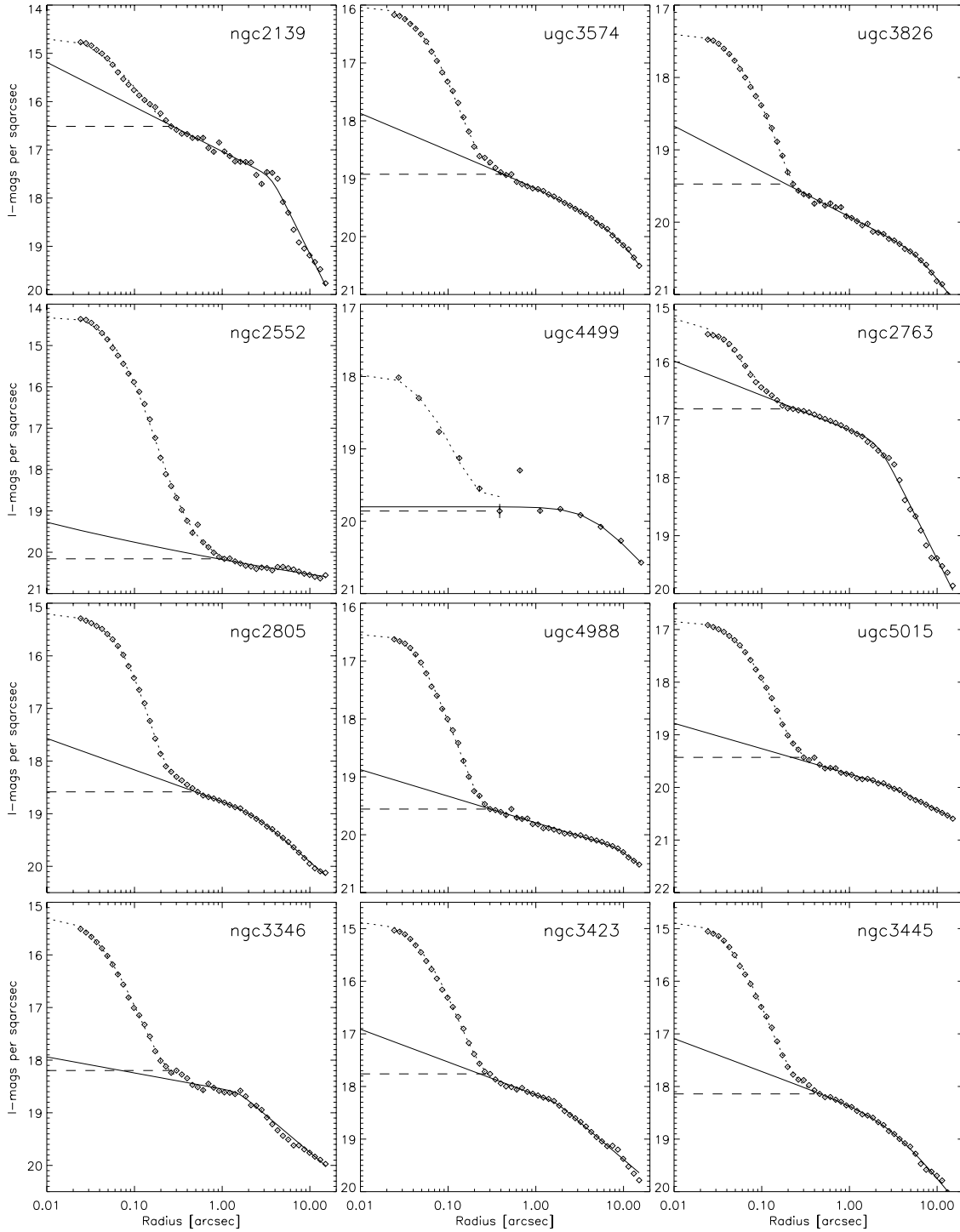


FIG. 3.—Continued

then has $M/L_I \approx 0.016$ and $M = 2.6 \times 10^4 M_\odot$, whereas for an old cluster with an age of 5 Gyr, one has $M/L_I \approx 0.43$ and $M = 6.9 \times 10^5 M_\odot$ (Leitherer et al. 1999). Our ongoing spectroscopic program to derive cluster ages for many of the sample galaxies promises to remove this ambiguity.

Photometry of the off-nuclear clusters in the low surface brightness disks of the group 2 galaxies, e.g., in UGC 12082 or ESO 187-51, shows that we can easily detect clusters as faint as $M_I = -8$. However, none of the galaxies in group 2 shows any evidence for *nuclear* clusters in this luminosity

range. This demonstrates that the low-luminosity cutoff in Figure 5 (*right panel*) around $M_I = -9$ is probably real.

2.5. The Size of Nuclear Star Clusters

To derive physically meaningful information about the structural properties of nuclear clusters, such as the half-light radius or the core radius in a King model, the observed SBPs have to be corrected for the instrumental PSF. Since the clusters in most cases are not much more extended than

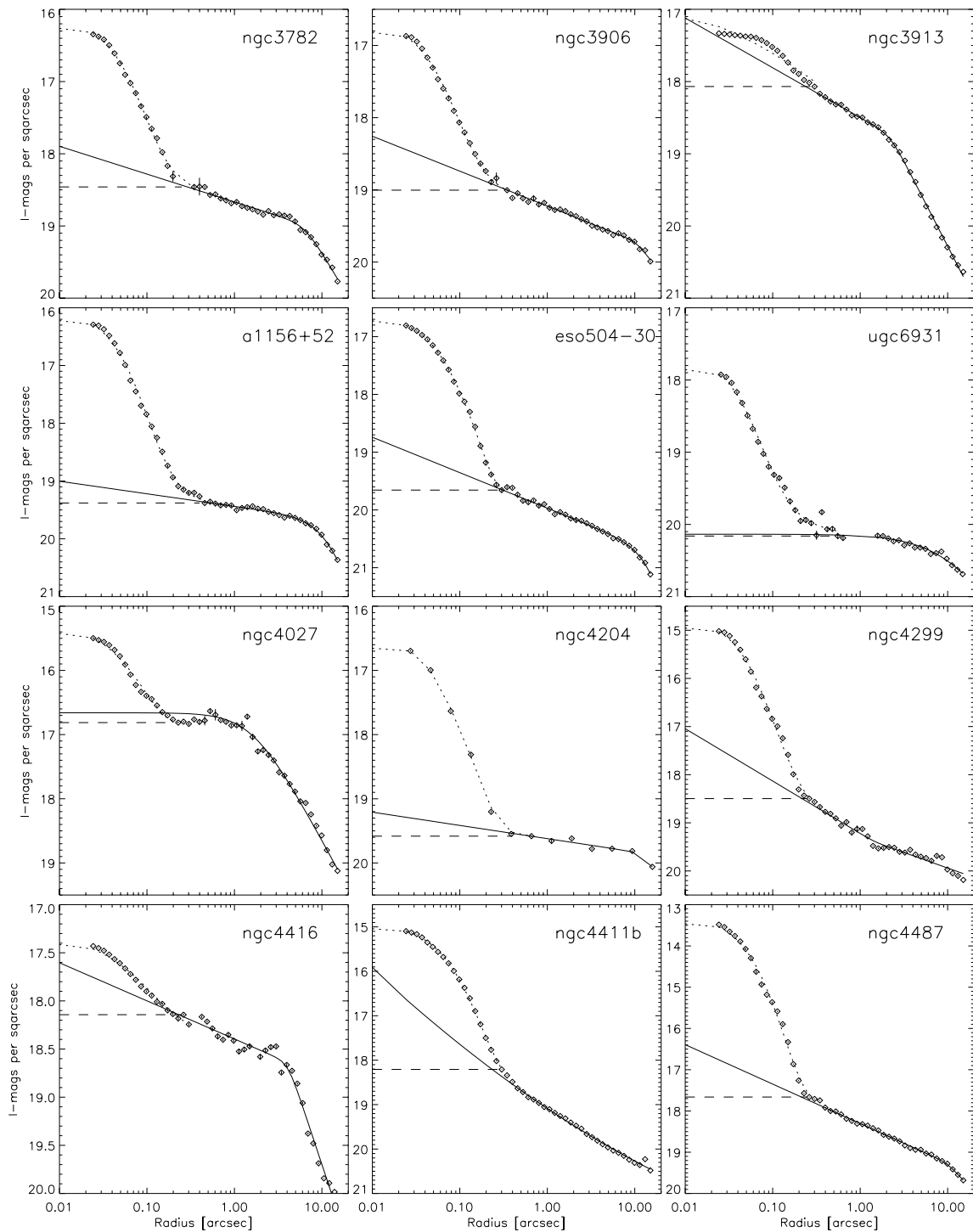


FIG. 3.—Continued

the *HST* PSF and the shape of the PSF is rather complex because of its extended wings, the deconvolution is a nontrivial task, and we defer it to a later paper (Sarzi et al. 2002).

For now, we list in Table 2 a simple measure of the nuclear cluster sizes, namely, the half-width at half maximum (HWHM); i.e., the radius at which the *observed* surface brightness drops to half its peak value. These were derived using simple linear interpolation between the two data points in the SBP that bracket half the peak value of the surface brightness. The listed values can be compared to those for the *HST* PSF. We constructed a PSF model from

the Tiny Tim software package (Krist & Hook 2001) for the PC chip and the F814W filter and performed an identical isophotal fit. The resulting HWHM was $0''.032$. For comparison, an identical analysis for a bright star in the image of the galaxy NGC 6509 yields $0''.036$. Both values are smaller than those listed in Table 2, which confirms that the nuclear clusters are indeed resolved.

Figure 6 (*left panel*) contains a histogram of the angular HWHM distribution that is strongly peaked around $0''.06$. We caution that the complexity of the *HST* PSF (which is only poorly represented by a single Gaussian) makes unreli-

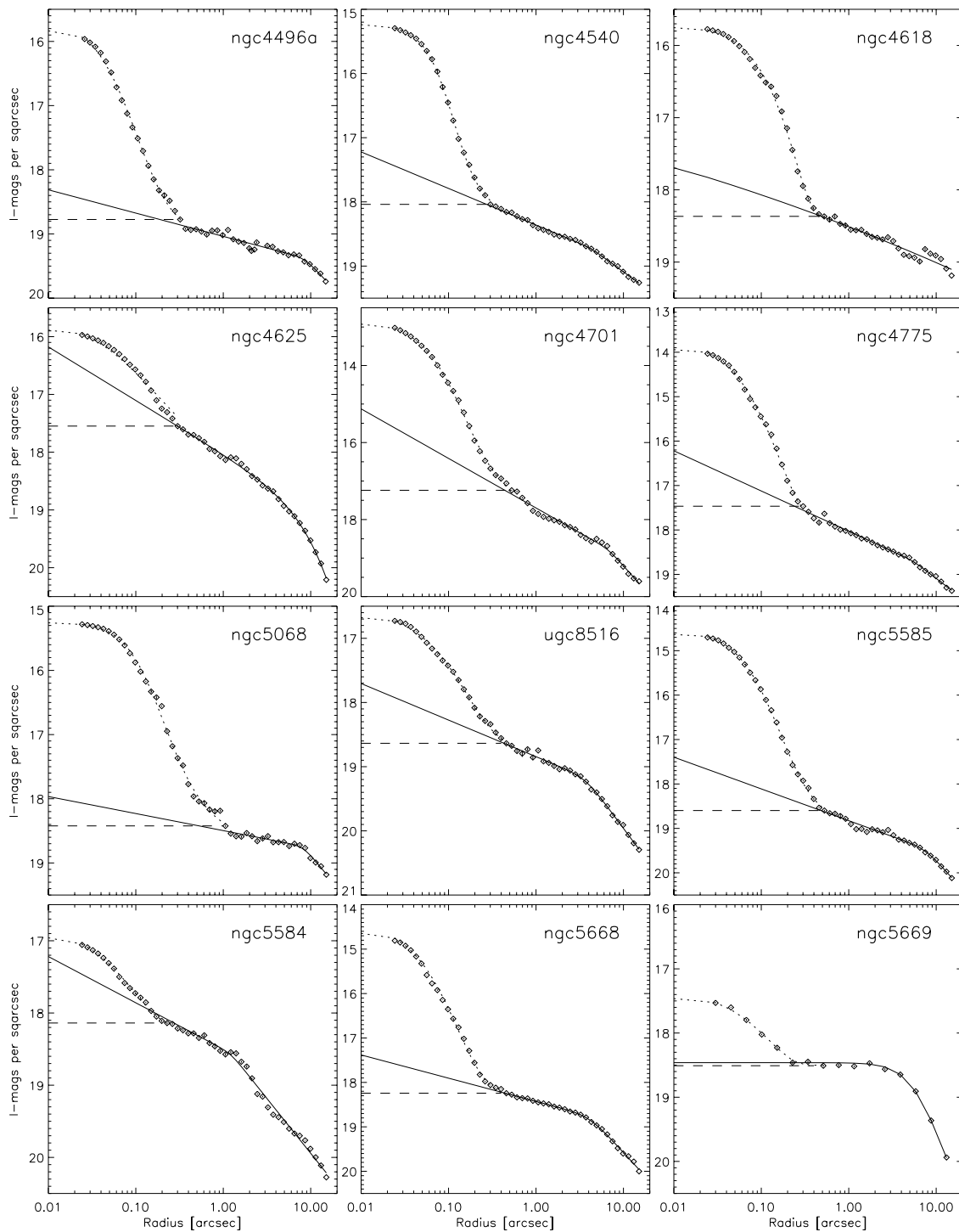


FIG. 3.—Continued

able the simple approach of quadratically subtracting the HWHM of the PSF from the observed one to obtain a measure of the intrinsic cluster size. Nevertheless, it is already clear from this simple analysis that the clusters are very compact, with typical intrinsic HWHM values of around 5 pc (Fig. 6, *right panel*).

As a whole, the nuclear clusters appear to be a very homogeneous class, not only in their luminosity but also in their structural parameters. The absence of unresolved nuclear sources in late-type galaxies—as suggested by this prelimi-

nary analysis—suggests that any accretion-powered emission from active galactic nuclei is optically weak in most galaxies of late Hubble types.

3. DISCUSSION

3.1. *Are the Clusters Truly Nuclear?*

The question of whether the clusters are indeed located at the photometric centers of their respective host galaxies is

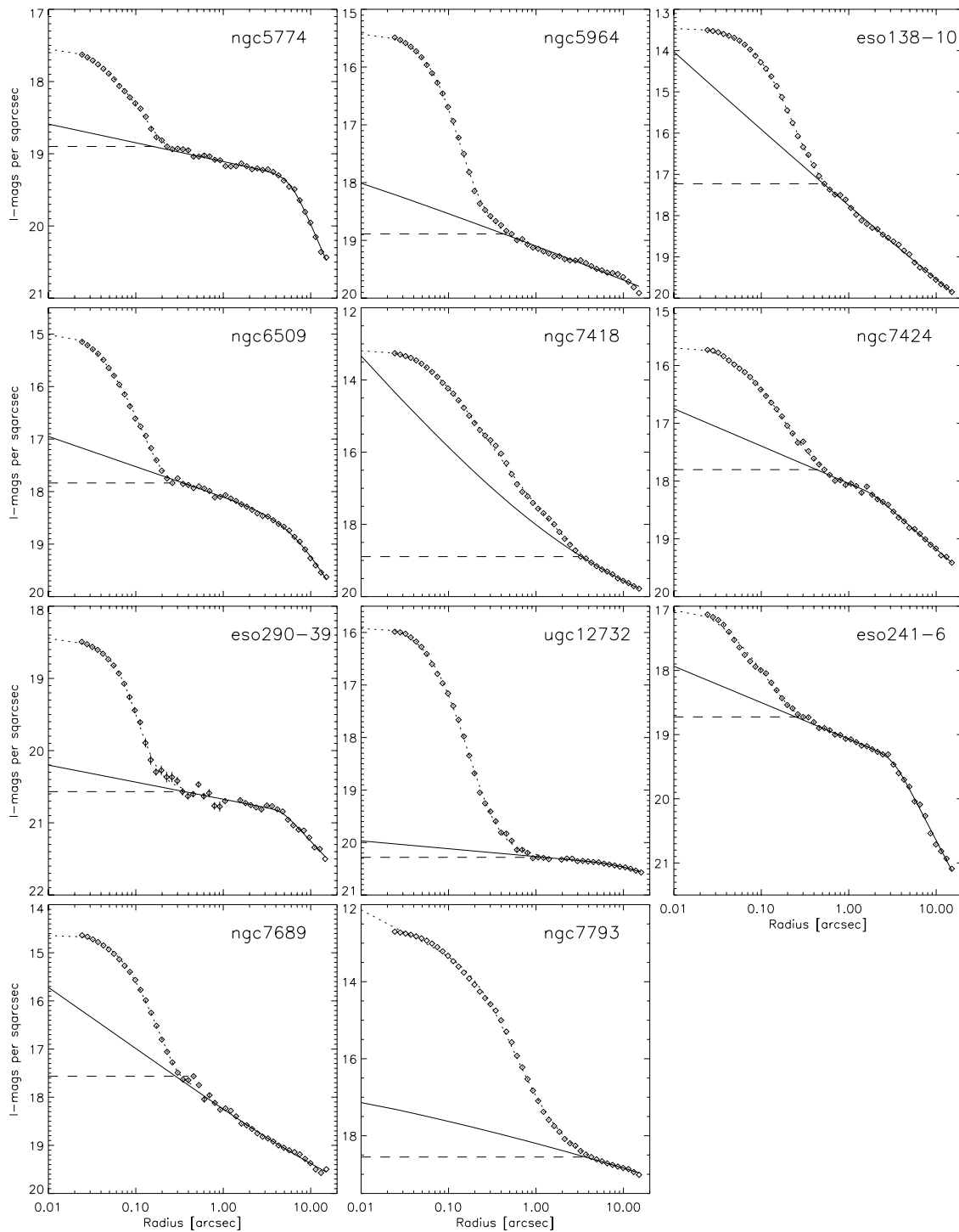


FIG. 3.—Continued

not easily answered because the term “photometric center” is not well defined itself. For our analysis, we have defined the photometric center as the average isophote center of our *ellipse* fitted results for radii between $2''$ (well beyond the extent of the cluster) and that of the outermost fitted ellipse—in most cases around $15''$. For the median distance of our sample, this radial range corresponds to linear scales between 200 pc and 1.5 kpc. If present, a stellar bar is likely to dominate the luminosity within this range, but since in the absence of close interactions a bar should be symmetric

with respect to the dynamical center, its photocenter is likely a good measure of the true galaxy nucleus.

Figure 7 (*top left panel*) shows a histogram of the projected angular distance between the position of the presumed nuclear cluster and the galaxy photocenter according to the definition above. About 75% (45 out of 59) of clusters lie within $1''$ from the photocenter. This angular separation corresponds to about 90 pc at the median distance of our sample (19 Mpc). In this representation, some clusters appear to be well separated from the galaxy center. How-

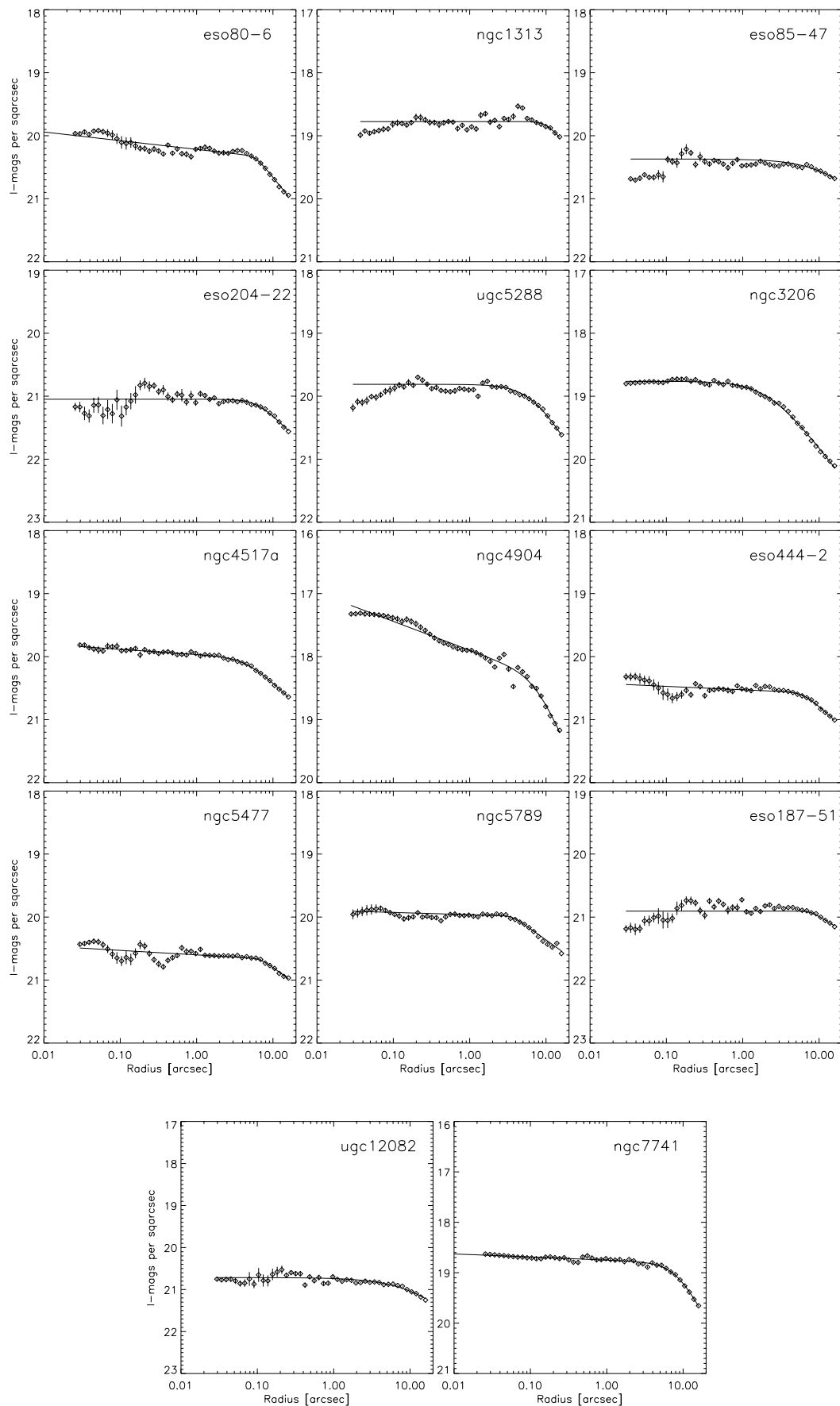


FIG. 4.—Same as Fig. 3, but for the 14 galaxies in group 2 (without evidence for a nuclear cluster) for which the isophotal fit was successful

TABLE 2
NUCLEAR CLUSTER PROPERTIES

Galaxy (1)	Distance (Mpc) (2)	HWHM (arcsec) (3)	HWHM (pc) (4)	R_n (arcsec) (5)	m_I (mag) (6)	M_I (mag) (7)	μ_0 (mag arcsec ⁻²) (8)	Type of Fit (9)
NGC 275	24.0	0.054	6.3	0.5	19.47 ± 0.01	-12.54	15.312	u
NGC 300	2.2 ^a	0.133	1.4	2.5	15.29 ± 0.40	-11.43	13.651	u
NGC 337a.....	14.3	0.058	4.0	0.6	20.94 ± 0.01	-10.02	17.144	u*
NGC 428	16.1	0.046	3.6	0.9	17.95 ± 0.01	-13.15	13.875	u
NGC 450	25.6	0.112	13.3	0.4	20.13 ± 0.17	-11.90	16.584	u
ESO 80-6.....	17.5	fc
NGC 600	25.2	0.057	7.0	0.3	19.92 ± 0.03	-12.16	15.712	u
NGC 853	20.2	0.054	5.3	0.25	19.90 ± 0.04	-11.68	15.515	u
NGC 1042.....	18.2	0.052	4.6	0.2	18.40 ± 0.29	-12.95	13.464	u
NGC 1313.....	4.4 ^b	fc
ESO 358-5.....	20.1	0.055	5.4	1.0	20.10 ± 0.06	-11.44	16.358	u*
ESO 418-8.....	14.1	0.052	3.6	0.3	20.54 ± 0.01	-10.24	16.154	u
NGC 1493.....	11.4	0.058	3.2	0.5	17.17 ± 0.03	-13.13	13.259	u
ESO 202-41.....	19.9	0.059	5.7	0.4	22.51 ± 0.03	-9.01	18.277	u*
ESO 85-47.....	16.9	fc
ESO 204-22.....	14.4	fc
NGC 2139.....	23.6	0.066	7.5	0.25	19.28 ± 0.29	-12.65	14.652	u
UGC 3574.....	23.4	0.065	7.4	0.5	20.04 ± 0.18	-11.90	16.063	u
UGC 3826.....	27.8	0.074	10.0	0.2	21.60 ± 0.02	-10.76	17.375	u
NGC 2552.....	9.9	0.053	2.6	1.0	18.04 ± 0.01	-12.04	14.220	u
UGC 4499.....	12.5	0.072	4.4	0.3	21.97 ± 0.63	-8.59	17.902	u*
NGC 2763.....	25.3	0.067	8.2	0.2	20.59 ± 0.35	-11.56	15.350	u
NGC 2805.....	28.1	0.060	8.2	0.5	19.02 ± 0.06	-13.32	14.987	u
UGC 4988.....	24.2	0.054	6.4	0.3	20.76 ± 0.04	-11.20	16.397	u
UGC 5015.....	25.7	0.065	8.2	0.3	20.71 ± 0.01	-11.37	16.686	u
UGC 5288.....	8.0	fc
NGC 3206.....	19.7	fc
NGC 3346.....	18.8	0.042	3.8	0.3	19.64 ± 0.01	-11.78	15.106	u
NGC 3423.....	14.6	0.057	4.1	0.3	19.04 ± 0.05	-11.84	14.876	u
NGC 3445.....	32.1	0.051	7.9	0.4	19.12 ± 0.10	-13.42	14.794	u
NGC 3782.....	13.5	0.055	3.6	0.25	20.61 ± 0.01	-10.07	16.134	u
NGC 3906.....	16.7	0.059	4.8	0.3	21.15 ± 0.11	-10.01	16.759	u
NGC 3913.....	17.0	0.255	21.0	0.3	21.22 ± 0.07	-9.96	17.256	u
A 1156 + 52.....	18.7	0.055	5.0	0.4	20.43 ± 0.01	-10.98	16.19	u
ESO 504-30.....	23.9	0.056	6.5	0.3	20.70 ± 0.05	-11.33	16.522	u
UGC 6931.....	20.7	0.052	5.2	0.5	21.91 ± 0.12	-9.72	17.757	u'
NGC 4027.....	22.7	0.066	7.3	0.2	20.38 ± 0.22	-11.48	15.335	u
NGC 4204.....	13.8	0.066	4.5	0.4	20.51 ± 0.02	-10.26	16.590	u*
NGC 4299.....	16.8 ^c	0.051	1.1	0.25	19.46 ± 0.04	-11.73	14.912	u
NGC 4416.....	20.7	0.219	22.0	0.25	22.82 ± 0.64	-8.81	17.415	u'
NGC 4411B.....	19.1	0.062	5.8	0.3	18.89 ± 0.07	-12.57	14.892	u
NGC 4487.....	14.6	0.051	3.6	0.25	17.89 ± 0.01	-12.97	13.391	u
NGC 4496A.....	25.3	0.048	6.0	0.3	20.08 ± 0.02	-11.99	15.631	u'
NGC 4517A.....	22.2	fc
NGC 4540.....	19.8	0.069	6.6	0.3	19.25 ± 0.02	-12.29	15.098	u
NGC 4618.....	10.7	0.098	5.1	0.5	18.74 ± 0.06	-11.45	15.668	u
NGC 4625.....	11.7	0.097	5.5	0.3	19.76 ± 0.08	-10.61	15.803	u
NGC 4701.....	11.0	0.044	2.4	0.5	16.81 ± 0.07	-13.45	12.641	u
NGC 4775.....	22.4	0.056	6.1	0.3	18.04 ± 0.05	-13.77	13.852	u
NGC 4904.....	17.2	fc
A 1301-03.....	19.7	ngf
IC 4182	7.4	ngf
ESO 444-2.....	22.1	fc
NGC 5068.....	8.7	0.106	4.5	1.0	17.55 ± 0.05	-12.34	15.194	u
UGC 8516.....	16.5	0.089	7.2	0.4	20.18 ± 0.09	-10.97	16.615	u
ESO 510-59.....	32.4	ngf
NGC 5477.....	8.1	fc
NGC 5585.....	8.2	0.063	2.5	0.5	18.24 ± 0.03	-11.35	14.531	u
NGC 5584.....	24.2	0.075	8.8	0.2	22.53 ± 0.58	-9.47	16.837	u
NGC 5789.....	28.6	fc
NGC 5668.....	23.8	0.054	6.3	0.4	18.86 ± 0.06	-13.10	14.757	u
NGC 5669.....	21.2	0.123	12.6	0.25	21.66 ± 0.01	-10.03	17.354	u*
NGC 5774.....	23.5	0.073	8.3	0.2	21.97 ± 0.05	-9.97	17.369	u

TABLE 2—*Continued*

Galaxy (1)	Distance (Mpc) (2)	HWHM (arcsec) (3)	HWHM (pc) (4)	R_u (arcsec) (5)	m_I (mag) (6)	M_I (mag) (7)	μ_0 (mag arcsec ⁻²) (8)	Type of Fit (9)
NGC 5964.....	22.2	0.056	6.1	0.5	19.22 ± 0.06	-12.62	15.210	u
ESO 138-10.....	13.5	0.085	5.6	0.5	16.68 ± 0.13	-14.40	13.367	u
NGC 6509.....	27.5	0.043	5.8	0.25	19.49 ± 0.07	-13.08	14.752	u
NGC 6946.....	5.5 ^c	ngf
ESO 187-51.....	16.5	fc
UGC 12082.....	13.9	fc
ESO 290-39.....	19.1	0.070	6.5	0.3	22.52 ± 0.01	-8.92	18.261	u'
NGC 7418.....	18.4	0.065	5.8	3.0	15.12 ± 0.22	-16.23	13.027	u
NGC 7424.....	10.9	0.097	5.1	0.5	18.80 ± 0.05	-11.41	15.650	u
UGC 12732.....	12.4	0.067	4.0	1.0	19.35 ± 0.01	-11.29	15.888	u'
ESO 241-6.....	17.4	0.056	4.7	0.3	21.30 ± 0.15	-9.93	16.884	u
NGC 7689.....	24.9	0.080	9.6	0.4	18.26 ± 0.12	-13.75	14.576	u
NGC 7741.....	12.5	fc
NGC 7793.....	3.3 ^d	0.096	1.5	4.0	14.00 ± 0.03	-13.64	12.551	u

NOTE.—Col. (1): Object name. Col. (2): Distance, derived from the recession velocity in Col. (4) of Table 1 and assuming $H_0 = 70$ km s⁻¹, if not noted otherwise. Cols. (3) and (4): Angular and physical observed HWHM of the nuclear cluster (i.e., not corrected for PSF convolution). The conversion assumes the distances listed in Col. (2). Col. (5): Aperture radius used to derive cluster luminosity. Col. (6): Apparent I -band magnitude of the nuclear cluster. Listed is the average value for the two background models, as described in § 2.4, and half their difference as the uncertainty. Col. (7): Absolute I -band magnitude of the nuclear cluster, corrected for Galactic extinction as listed in Col. (7) of Table 1. The distance modulus was derived from the distances in Col. (2). Col. (8): Peak observed I -band surface brightness in a $0''.0455$ pixel² (i.e., not corrected for PSF convolution). Col. (9): Type of the isophotal fit: “u” indicates unconstrained, sometimes with increased isophote spacing (*asterisk*) or over two separate radial ranges (*prime*); “fc” indicates fixed ellipse center and ellipticity; “ngf” indicates no good fit.

^a From Freedman et al. 1992.

^b From de Vaucouleurs 1963.

^c From Tully 1988.

^d From Carignan 1985.

ever, we caution that in many galaxies of our sample, the photocenter is poorly defined and its position very uncertain.

In order to visualize the uncertainties in the photocenter positions, we show in Figure 7 (*top right panel*) a plot of the projected offset between photocenter and nuclear cluster for

all galaxies in group 1. Here the sizes of the crosses indicate the standard deviation σ in the image x - and y -directions of the isophote centers measured from isophotes at radii $\geq 2''$. If one assumes that the isophote centers are subject to random measurement errors, then the error in the photocenter position should be σ/\sqrt{n} , where n is the number of iso-

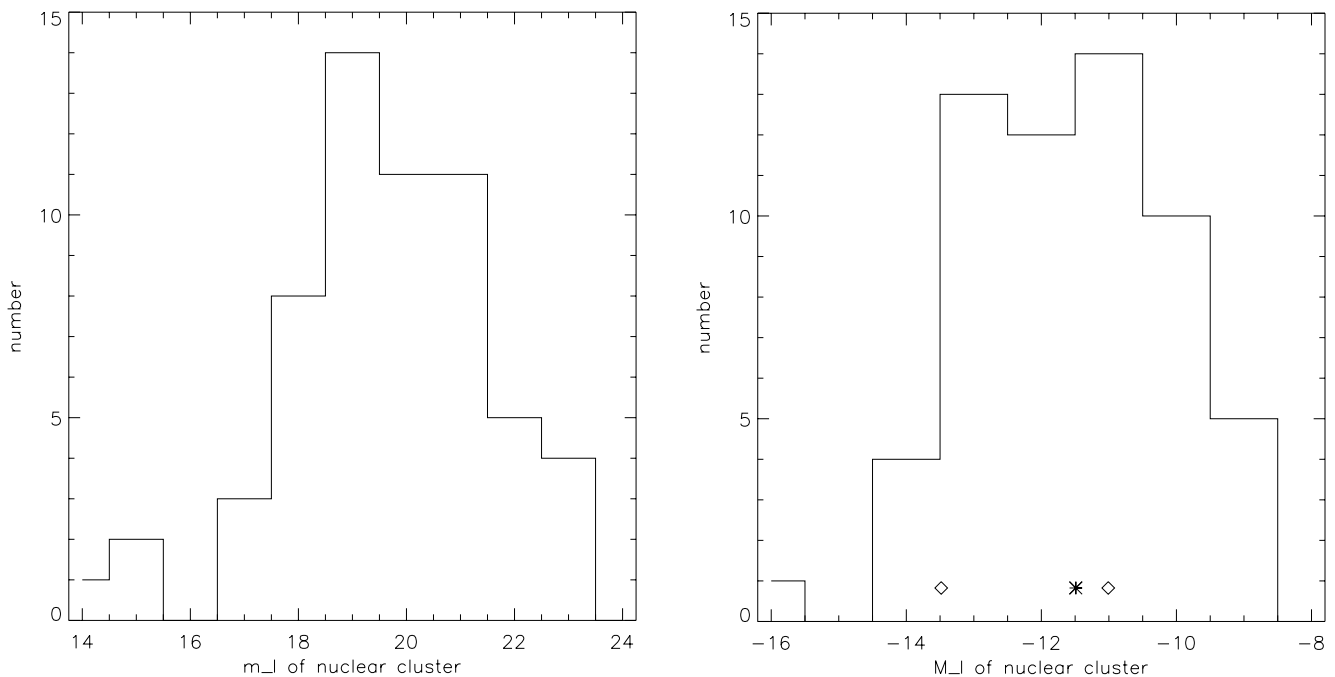


FIG. 5.—Histogram of apparent (*left*) and absolute (*right*) I -band magnitudes of all identified nuclear clusters. Also shown are the median absolute luminosity of the sample (*asterisk*) and the luminosity of a cluster with 10^6 and $10^7 L_\odot$, respectively (*diamonds*).

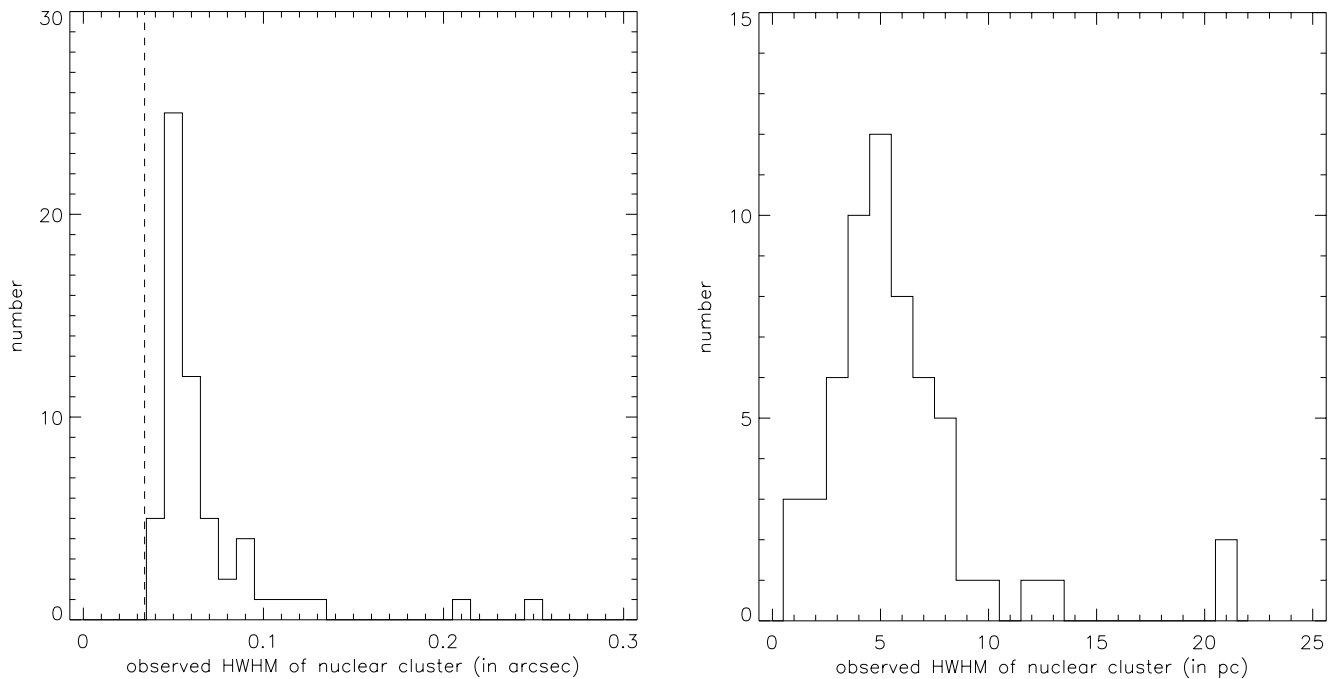


FIG. 6.—Angular (*left*) and linear (*right*) observed HWHM radii (i.e., not corrected for PSF convolution) of all identified nuclear clusters. Vertical dashed line in left panel denotes the HWHM radius of the F814W PSF.

photos. However, the isophotal fits are clearly influenced by dust lanes, extended star formation, or other asymmetries that vary with isophote radius and thus make the determination of the photocenter of an individual galaxy subject to systematic uncertainties. We therefore have conservatively estimated the error in the photocenter position to equal σ , without dividing by \sqrt{n} .

The fact that this estimate is indeed a conservative one is demonstrated in Figure 7 (*bottom panel*), which shows the cumulative distribution of cluster positions inside a certain number of standard deviations. The observed sample is compared to the expected curve for a two-dimensional normal (i.e., Gaussian) error distribution. The observed distribution is narrower than the prediction, which indicates that we have somewhat overestimated our errors in determining the photocenter.

While this analysis does not prove that each individual cluster does indeed occupy the true nucleus of its host galaxy, the results demonstrate that the majority of clusters are—within the errors—located at or very near the photometric center. In the absence of any kinematical information, it is reasonable to assume that the photocenter coincides with the dynamical center. We therefore conclude that these clusters can rightfully be called “nuclear.”

3.2. Are Nuclear Clusters Special?

One of the most interesting results from *HST* imaging has been the discovery of extremely luminous, compact young star clusters in a variety of starburst environments, including merging galaxies (Conti & Vacca 1994; Whitmore et al. 1999), dwarf galaxies (Hunter, O’Connell, & Gallagher 1994; Calzetti et al. 1997), and in the circumnuclear rings of nearby spiral galaxies (Barth et al. 1995; Buta et al. 2000; Maoz et al. 2001). Prior to *HST*, only a few objects of this type were known to exist (Arp & Sandage 1985; Melnick, Moles, & Terlevich 1985); the severe crowding in most star-

bursts made it impossible to resolve the individual clusters in ground-based images. Such “super star clusters” apparently form preferentially during extreme episodes of violent star formation and may be the basic building blocks of starbursts. Barely resolved by *HST*, they have effective radii of only 2–4 pc and luminosities that range as high as $M_V = -14$ to -15 mag. The small radii, high luminosities, and presumably high masses of these clusters have led to suggestions that they may remain as bound systems and therefore could be present-day versions of young globular clusters (e.g., Ho & Filippenko 1996).

The nuclear clusters discovered in our survey bear a close resemblance to off-nuclear super star clusters. Although we do not yet have definitive size measurements for our sources, the observed HWHM values range from ~ 1 to 10 pc, with a median value of ~ 5 pc; this is consistent with the sizes of super star clusters. Similarly, the optical absolute magnitudes of the nuclear clusters lie comfortably within the luminosity function of super star clusters.

4. CONCLUSIONS

We have presented a catalog of *HST*/WFPC2 *I*-band images of an unbiased sample of 77 nearby late-type spiral galaxies with low inclination. From an isophotal analysis of the images, we demonstrate that about 75% of the sample galaxies host a compact luminous stellar cluster at or very close to their photocenter. These clusters often are completely isolated from other comparable structures, emphasizing that even in the relatively shallow potential wells of late-type galaxy disks, the center is well-defined and has a unique star formation history. From analytical fits to the surface brightness profiles, we determine the flux attributable to the cluster. The distribution of absolute cluster luminosities has a FWHM of 4 mag and a median value of

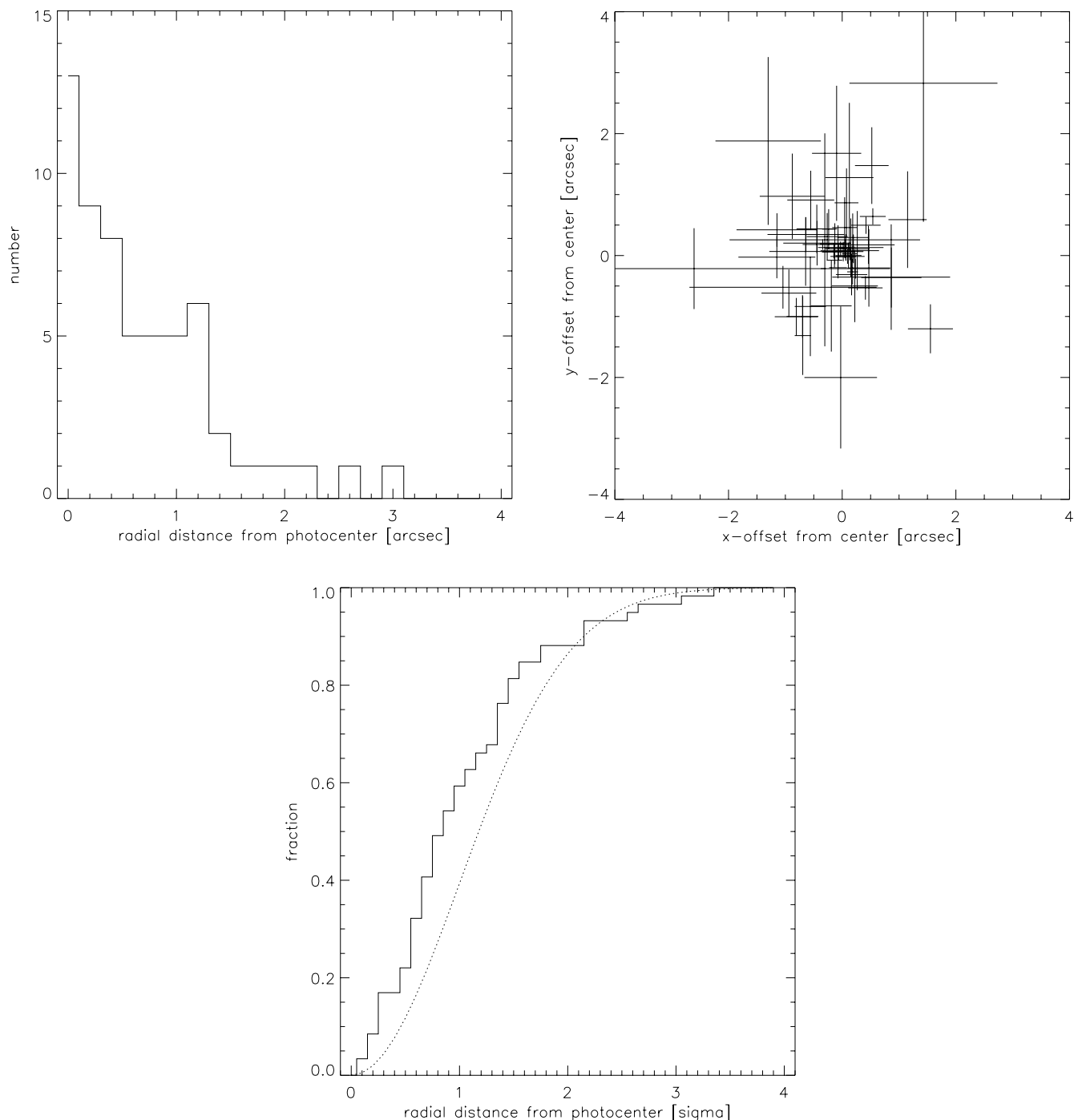


FIG. 7.—(left) Distribution of projected distances between nuclear cluster position and the average isophote center between $2''$ and $15''$. (right) Projected position of all nuclear clusters, relative to the photocenter of their respective host galaxy. Size of the crosses denotes the 1σ scatter in the isophote centers. (bottom) Cumulative distribution of projected distance between cluster and photocenter (solid curve) compared to the expected curve for a two-dimensional Gaussian error distribution (dotted curve).

$M_I = -11.5$, comparable to young super star clusters in starbursting galaxies. Together with initial estimates of their size distribution, this suggests that nuclear clusters in spiral galaxies of the latest Hubble types are a fairly homogenous class of objects. The data set is a representative survey of late-type spiral galaxies in the local universe and as such yields a valuable source catalog for spectroscopic follow-up observations that are needed to further constrain the star formation history of nuclear clusters. We have begun such a follow-up program with both *HST* and ground-based observatories.

The anonymous referee provided useful comments that helped improve this paper. Support for proposal 8599 was provided by NASA through a grant from the Space Telescope Science Institute, which is operated by the Association for Research in Astronomy, Inc., under NASA contract NAS 5-26555. This research has made use of the NASA/IPAC Extragalactic Database, which is operated by the Jet Propulsion Laboratory, California Institute of Technology, under contract with NASA. It has also benefited greatly from use of the Lyon-Meudon Extragalactic Database.

REFERENCES

- Arp, H., & Sandage, A. 1985, *AJ*, 90, 1163
- Barth, A. J., Ho, L. C., Filippenko, A. V., & Sargent, W. L. W. 1995, *AJ*, 110, 1009
- Böker, T., van der Marel, R. P., Mazzuca, L., Rix, H.-W., Rudnick, G., Ho, L., & Shields, J. C. 2001, *AJ*, 121, 1473
- Böker, T., van der Marel, R. P., & Vacca, W. D. 1999, *AJ*, 118, 831
- Böker, T., et al. 2002a, in preparation
- . 2002b, in preparation
- Buta, R., Treuthardt, P. M., Byrd, G. G., & Crocker, D. A. 2000, *AJ*, 120, 1289
- Byun, Y.-I., et al. 1996, *AJ*, 111, 1889
- Calzetti, D., Meurer, G., Bohlin, R. C., Garnett, D., Kinney, A. L., Leitherer, C., & Storchi-Bergmann, T. 1997, *AJ*, 114, 1834
- Cardelli, J. A., Clayton, G. C., & Mathis, J. S. 1989, *ApJ*, 345, 245
- Carignan, C. 1985, *ApJS*, 58, 107
- Carollo, C. M. 1999, *ApJ*, 523, 566
- Carollo, C. M., Stiavelli, M., de Zeeuw, P. T., & Mack, J. 1997, *AJ*, 114, 2366
- Carollo, C. M., Stiavelli, M., de Zeeuw, P. T., Seigar, M., & Dejonghe, H. 2001, *ApJ*, 546, 216
- Carollo, C. M., Stiavelli, M., & Mack, J. 1998, *AJ*, 116, 68
- Conti, P. S., & Vacca, W. D. 1994, *ApJ*, 423, L97
- de Vaucouleurs, G. 1963, *ApJ*, 137, 720
- de Vaucouleurs, G., de Vaucouleurs, A., Corwin, H., Buta, R. J., Paturel, G., & Fouque, P. 1991, *Third Reference Catalog of Bright Galaxies* (New York: Springer)
- Freedman, W. L., Madore, B. F., Hawley, S. L., Horowitz, I. K., Mould, J., Navarrete, M., & Sallmen, S. 1992, *ApJ*, 396, 80
- Gelatt, A. E., Hunter, D. A., & Gallagher, J. S. 2001, *PASP*, 113, 142
- Ho, L. C., & Filippenko, A. V. 1996, *ApJ*, 472, 600
- Holtzman, J. A., Burrows, J., Casertano, S., Hester, J. J., Trauger, J. T., Watson, A. M., & Worthey, G. 1995, *PASP*, 107, 1065
- Hunter, D. A., O'Connell, R. W., & Gallagher, III, J. S. 1994, *AJ*, 108, 84
- Kormendy, J., & McClure, R. D. 1993, *AJ*, 105, 1793
- Krabbe, A., et al. 1995, *ApJ*, 447, L95
- Krist, J., & Hook, R. 2001, *The Tiny Tim User's Guide* (v. 6.0; Baltimore: STScI)
- Lauer, T. R., Faber, S. M., Ajhar, E. A., Grillmair, C. J., & Scowen, P. A. 1998, *AJ*, 116, 2263
- Lauer, T. R., et al. 1995, *AJ*, 110, 2622
- Leitherer, C., et al. 1999, *ApJS*, 123, 3
- Maoz, D., Barth, A. J., Ho, L. C., Sternberg, A., & Filippenko, A. V. 2001, *AJ*, 121, 3048
- Matthews, L. D., & Gallagher, III, J. S. 1997, *AJ*, 114, 1899
- Matthews, L. D., et al. 1999, *AJ*, 118, 208
- Melnick, J., Moles, M., & Terlevich, R. 1985, *A&A*, 149, L24
- O'Connell, R. W., Gallagher, J. S., Hunter, D. A., & Colley, W. A. 1995, *ApJ*, 446, L1
- Paturel, G., & Petit, C. *Lyon-Meudon Extragalactic Database* (Lyon: Lyon Claude-Bernard Univ.)
- Phillips, A. C., Illingworth, G. D., MacKenty, J. W., & Franx, M. 1996, *AJ*, 111, 1566
- Salpeter, E. E. 1955, *ApJ*, 121, 161
- Sandage, A., & Tammann, G. 1990, *ApJ*, 365, 1
- Sarzi, M., et al. 2002, in preparation
- Schinnerer, E., Eckard, A., & Tacconi, L. J. 2001, *ApJ*, 549, 254
- Schlegel, D. J., Finkbeiner, D. P., & Davis, M. 1998, *ApJ*, 500, 525
- Tully, R. B. 1988, *Nearby Galaxies Catalog* (Cambridge: Cambridge Univ. Press)
- Whitmore, B. C., Zhang, Q., Leitherer, C., Fall, S. M., Schweizer, F., & Miller, B. W. 1999, *AJ*, 118, 1551